npj | Flexible Electronics

www.nature.com/npjflexelectron

REVIEW ARTICLE OPEN

Energy autonomous electronic skin

Carlos García Núñez[1,2], Libu Manjakkal[1] and Ravinder Dahiya[1]

Energy autonomy is key to the next generation portable and wearable systems for several applications. Among these, the electronic-skin or *e*-skin is currently a matter of intensive investigations due to its wider applicability in areas, ranging from robotics to digital health, fashion and internet of things (IoT). The high density of multiple types of electronic components (e.g. sensors, actuators, electronics, etc.) required in *e*-skin, and the need to power them without adding heavy batteries, have fuelled the development of compact flexible energy systems to realize self-powered or energy-autonomous *e*-skin. The compact and wearable energy systems consisting of energy harvesters, energy storage devices, low-power electronics and efficient/wireless power transfer-based technologies, are expected to revolutionize the market for wearable systems and in particular for *e*-skin. This paper reviews the development in the field of self-powered *e*-skin, particularly focussing on the available energy-harvesting technologies, high capacity energy storage devices, and high efficiency power transmission systems. The paper highlights the key challenges, critical design strategies, and most promising materials for the development of an energy-autonomous *e*-skin for robotics, prosthetics and wearable systems. This paper will complement other reviews on *e*-skin, which have focussed on the type of sensors and electronics components.

npj Flexible Electronics (2019)3:1 ; https://doi.org/10.1038/s41528-018-0045-x

INTRODUCTION

An electronic-skin or *e*-skin is an artificial smart skin consisting of multiple sensors distributed either along the same surface (Fig. 1a) or stacked as shown in Fig. 1b. With various sensors spread over a large area, mimicking some of the features of human skin, the *e*-skin could bestow robots and prostheses with sense of touch.[1–5] Moreover, the *e*-skin can also act as a 'second skin' in humans,[6] i.e. sticking onto the body surface, with sensors augmenting the natural sensory capacity by measuring various body parameters (e.g. blood pressure, body temperature, heartbeat, etc.)[7–13] or ambient parameters (e.g. gases, chemical, materials, radiation, etc.).[14–16] The *e*-skin also require integration of large number of sensing/electronic components on flexible and conformal surfaces,[11,17] as evident from the growing trend of high density of sensors in medical patches,[9,18–24] active-matrix for touch screens[25] and tactile sensitive artificial skins for robots/prosthesis.[1,8] This also leads to a higher demand of energy, requiring energy harvesting/storage devices with high energy densities and capacities. In addition, the development of high-performance energy transfer technologies is also needed, comprising new strategies to deliver energy, e.g. wireless protocols. A self-powered *e*-skin, also called here as energy-autonomous *e*-skin, can harvest sufficient energy from the ambient to power all its sensors and electronic components, and storing the excess of energy for future use. In this scenario, *e*-skin could have continuous and stable operation, even during short absence of energy sources. In this sense, the energy autonomy of *e*-skin will also improve the acceptance of flexible and wearable systems using this technology.

Currently, the energy requirements of *e*-skin are met with bulky batteries or energy harvesters (Fig. 1c) that do not always produce sufficient energy, and also affect the portability and overall wearability of the *e*-skin. The batteries offer a limited life span and short charging/discharging cyclic stability and durability, risky overheating effects, and are often heavy.[26] Because of the need, and currently the lack of suitable solutions, significant efforts have been devoted during the last decades to develop alternative solutions such as light-weight *e*-skin (Fig. 1d) with wearable energy harvesters (e.g. photovoltaics, thermo-electricity, piezo-electricity and triboelectricity[1,27]) and energy storage devices (e.g. flexible batteries (Fig. 1e)[28,29] and supercapacitors[30]). Considering the key role of energy, this paper focuses on the *e*-skin requirements and potential solutions with integrated energy harvesting/storing technologies. Among all potential energy sources, light, thermal and mechanical energies, have demonstrated excellent performance for powering *e*-skin due to abundance in the environments where the *e*-skin could be used. In addition, the chemical energy from various human body fluids (e.g. tears, saliva, sweat, etc.) and biofuels are attracting interest as promising energy sources for powering *e*-skin in wearables.[31–34] The progresses in the field of energy-harvesting technologies include the fabrication of energy harvesters on rigid as well as non-conventional flexible/stretchable substrates, e.g. stretchable PV cells,[35] light thermocouple energy generators,[36] or flexible triboelectric energy nanogenerators.[37] In this regard, the future of *e*-skin is sometimes subjected to the success of energy harvesters and storage technologies developed on flexible/stretchable substrates. The performance of some of the above technologies is still far from the requirements for fully autonomous *e*-skin, i.e. an *e*-skin that can work continuous for 24 h with high stability and reliability. Low power conversion efficiency of technology developed on flexible substrates and discontinued energy supply are the two main drawbacks observed in energy harvesters based on light, mechanical and thermal energies. Although there are already some examples of continuous powering of *e*-skin,[38] the latest progress reported on

[1]Bendable Electronics and Sensing Technologies (BEST) Group, School of Engineering, University of Glasgow, G12 8QQ Glasgow, UK and [2]Scottish Universities Physics Alliance (SUPA), Institute of Thin Films, Sensors & Imaging (TFSI), University of the West of Scotland, Paisley PA1 2BE, UK
Correspondence: Ravinder Dahiya (ravinder.dahiya@glasgow.ac.uk)

Received: 14 June 2018 Accepted: 13 December 2018
Published online: 04 January 2019

Fig. 1 Multi-sensing and flexible electronic skin for robots and humans. 3D schema of a flexible *e*-skin with multiple electronic components (sensors, electronics, memory, energy harvesters, etc.) distributed **a** along the same surface or **b** stacked. Reprinted with permission from Dahiya et al.[211] Copyright © 2015, IEEE. The *e*-skin self-powered by **c** a bulky battery (reprinted with permission from Leonov et al.[54] Copyright © 2009, AIP Publishing) or **d**, **e** a light-weight wearable solar cell. Reprinted with permission from García Núñez et al.[1] Copyright © 2017, John Wiley and Sons. Reprinted with permission from Bauer et al.[3] Copyright © 2013, Springer Nature. **f** iCub robotic body and arm covered with *e*-skin (see inset). Reprinted with permission from Cannata et al.[49,53] The 3D reconstruction of a skin patch placed on **g** a container, and **h** a KUKA LWR arm. Reprinted with permission from Dahiya et al.[50] Copyright © 2013, IEEE. **i** Image of the prosthetic/robotic hand with *e*-skin.[8]

multi-sensing *e*-skin[7,39] and the reduction of the sensors and electronics size,[16,40–42] have drastically increased the energy requirements for this technology. Therefore, current challenges on energy-autonomous *e*-skin are not focused only on the discovery of new sources of energy (e.g. chemical and electrochemical energy[43]) and high-efficient energy-harvesting mechanisms (e.g. triboelectrics[44–47]), but also on the integration of different energy harvesting and storage technologies, resulting in a portable power pack.[38,48]

Prior to the discussion about the potential strategies to harvest, store and deliver energy to *e*-skin, it is important to mention the power requirements of this technology so that suitable energy could be explored. A large number of sensors and electronic components, made from different materials (e.g. graphene (Fig. 1d)),[1] piezoelectric polymers such as polyvinylidene fluoride (PVDF) (Fig. 1f–h)),[49,50] or transparent conductive oxides such as indium tin oxide (ITO) (Fig. 1i)[8]) are needed for various sensors in large-area *e*-skin for robots.[49,51] The power requirement multiplies

Fig. 2 Energy-autonomous electronic skin: potential energy sources. The schematic diagram of self-powered *e*-skin, comprising: (i) energy harvesting (light, mechanical, chemical and thermal energy), (ii) energy storage (batteries and supercapacitors) and (iii) examples of self-powered *e*-skin solutions. Energy harvesting: the illustration compiles the best performance energy harvesters and their corresponding energy outcome (i.e. power density) depending on the energy source (light,[66,73,81] mechanical,[98,103] chemical[32,33] and thermal energy[133,137]), highlighting successful devices exhibiting features including stretchability, lightweight, output powers and wearability. Energy storage: highlighting various flexible active electrodes that enhance the performance of LiBs[169,220–222] and textile/fibre/cloth-based supercapacitors[223–227] for wearable systems. Examples of self-powered *e*-skin solutions: the illustration shows representative examples of electronic devices continuously self-powered by various energy sources, including tactile *e*-skin for robots self-powered by sunlight (reprinted with permission from García Núñez et al.[1] Copyright © 2017, John Wiley and Sons), *e*-skin self-powered by a biofuel cell and integrated on a contact-lens (reprinted with permission from Falk et al.[34] Copyright © 2012 Elsevier B.V), wearable sensors self-powered by thermoelectric generators (reprinted with permission from Leonov et al.[54] Copyright © 2009, AIP Publishing), wearable *e*-patch for human health monitoring (reprinted with permission from Yang et al.[55] Copyright © 2009, American Chemical Society), multi-sensing *e*-skin on fabrics self-powered by piezoelectric generators (Reprinted with permission from Li et al.[56] Copyright © 2016, Springer Nature)

with the increasing number of sensing and associated electronic components. For example, the flexible printed circuit boards based *e*-skin, developed through ROBOSKIN research project (Fig. 1f),[52] to cover the body of a humanoid robot 'iCub' has about 1000 capacitive touch sensors,[53] requiring about 7.5 W to power the *e*-skin. This calculation considers the macroscopic sensing modules only. In reality the power consumption will be much higher if we reduce the size of sensors down to the micro- or even nano-scale, to mimic the touch sensitivity of human body (where an estimated 4.5×10^4 mechanoreceptors are present in about 1.5 m^2 area[8]) with increased the number of touch sensors. This number of sensors will be further going up if we also consider thermo-sensors, and chemical-sensors, etc. Likewise, the Hex-O-Skin made with off-the-self components requires 4.5 W.[51] For continuous operation of *e*-skin, the energy requirements can be high—particularly when robots are battery powered. In this regard, new materials such as graphene (Fig. 1d)[1] or ITO (Fig. 1i)[8] have demonstrated great potential as they require much lower power (~20 nW/cm^2 for graphene[1] and ~100 μW/cm^2 for ITO[8]). With these conditions, the power consumption of graphene-based *e*-skin to cover the 1.5 m^2 surface of a robot body will be of 3.9 μW, which is about six order of magnitude less than the off-the-shelf

components based on large-area tactile skins discussed above. This significantly low energy needed by latest *e*-skin makes it feasible to use ambient energy sources such as light, mechanical or thermal energies as potential sources to power *e*-skin (Fig. 2).

Figure 2 summarizes the state-of-the art energy harvesting and storage technologies successfully utilized in *e*-skin-like systems such as graphene-based tactile skin powered by sunlight,[1] a pulse oximeter powered by thermal energy from human body,[54] healthcare *e*-patch powered by human finger vibrations[55] and multi-sensing *e*-skin on fabrics powered by human arm actions.[56] The best reported performances (e.g. power density and capacity) are also shown in Fig. 2. The energy harvesting, and storage solutions presented in Fig. 2 show their suitability for a wide range of *e*-skin applications.

This paper is organized as follows: The following section presents the advances in the energy harvesting with particular focus on the solutions relevant to *e*-skin. This is followed by a discussion in the section 'Towards continuous energy supply: technologies for energy storage and wireless charging' on the energy storage and transmission technologies, including wireless energy transfer. Few examples of self-powered *e*-skin systems are presented in the section 'Self-powered *e*-skin'. The key challenges and potential solutions, critical design strategies, and most promising materials for the development of energy-autonomous *e*-skin have been discussed in the section 'Key challenges and potential solutions for future self-powered *e*-skin'. Finally, the conclusion and future outlook are given in the 'Discussion' section. With several reviews on *e*-skin[50,57,58] focussing on the sensing and electronics components only, in this paper, the discussion about the energy autonomy in *e*-skin will complement and strengthen the existing literature.

SOURCES OF ELECTRICAL ENERGY

In this section, we have compiled the most promising energy sources available in the ambient for self-powering of *e*-skin and other similar technologies presented in the section 'Self-powered *e*-skin'. The fundamental mechanism behind each type energy-harvesting method, their approximate energy budget, i.e. power conversion efficiency (PCE) and power density (PD), etc. are thoroughly discussed. Since several applications require *e*-skin to be flexible or to conform to 3D surfaces, the discussion here considers the energy-harvesting solutions with features such as bendability, conformability, wearability, stretchability, and compatibility to low-temperature fabrication procedures.

Light energy

Among all, solar energy is one of the most abundant renewable energies available from the environment. The solar energy that is provided to the earth surface during 1 h exceeds by far the energy consumed globally by humans in 1 year.[59] This is the main reason to consider light energy as a potential source for self-powered systems. A solar-powered *e*-skin integrated on the body of a robot would allow the robot to execute tasks in wide ranging environments, either on the Earth or in space, thanks to the great amount of energy supplied by the sun.

Photovoltaic (PV) materials that are typically used to transform sunlight energy into electricity are based on semiconductor solid-state thin films made of crystalline Si (c-Si), amorphous-Si (a-Si), polycrystalline-Si (poly-Si) and monocrystalline Si (mc-Si).[59] Flexible PV cells, which could meet the conformability requirements of *e*-skin, have also been fabricated successfully using a-Si (PCE ~ 8%),[60] and enormous effort is being put to fabricate the new generation of low-cost PV cells with higher PCE, lightweight, and using print technology. These technologies mainly include dye-sensitized PV cells and the PV cells based on organic materials, quantum dots and perovskites.[28,61–65] The lightweight, conformability, compatibility to low-temperature processing and to textile/fabrics like substrates of PV cells, mechanical strength, low-cost fabrication process, and biocompatibility (e.g. for *e*-skin applications on humans or animals) are also crucial properties for the use of PVs as energy source in portable and wearable self-powered *e*-skin.[61] For the sake of comparison, the PCE (obtained using an A.M. 1.5 solar illumination with 100 mW/cm^2 intensity) of various PV technologies discussed here is given in the corresponding subsections.

Semiconductor solid-state PV cells. Historically, crystalline silicon (c-Si) PV cells have dominated the PV market, occupying a share of about 93% in 2016.[59] This is mainly because of the existing manufacturing industry available for this material, its earth-abundance and high-performance PV effect in the sunlight electromagnetic range. However, it is believed that the potential increase of the PCE and PD and the reduction of the manufacturing cost of Si PV cells are getting saturated over the time.[59] Si and GaAs have shown the highest PCE (>25%) in single-junction configuration, above other semiconductor materials such as InP, GaInP, CdTe, CIGS, CIGS, CIS, Perovskite, CZTSSe and CZTS, which typically exhibit PCE below 25%.[27] Accordingly, Si and III-V PVs industry is evolving beyond the conventional single-junction-based PV cells, constrained by Shockley–Queisser limits to values below 30%, with new approaches such as multi-junction (MJ), intermediate band, and multiple-exciton generation (MEG) quantum-confined based PV cells which can potentially exceed those limits. Among all, GaInP/GaAs MJ-based PV cells have shown the highest PCE of 46% and exhibited PD up to 345 W/m^2 (Table 1).[66] In spite of the excellent performance demonstrated by these PV cells, their implantation on *e*-skin applications is not straightforward yet because of their poor mechanical properties, non-compatibility to low-temperature fabrication procedures, toxicity of some of the constituents, and complex fabrication. Although further investigations are still needed, some preliminary works reported in the literature demonstrate features such as portability, lightweight and flexibility in semiconductor solid-state-based PVs.[67] However, their performance is poorer than their rigid counterparts. The best flexible PV cells fabricated so far, based on III-V materials (in MJ configuration), exhibit a PCE up to 27.6% and a PD of 276 W/m^2.[67] These are promising results to power micro-/nano-electronics (see the section 'Self-powered e-skin'), for example, in a human inspired *e*-skin for humanoid (effective area: 1.45 m^2) or prosthetic hand (effective area: 0.019 m^2),[8] where generation of an estimated power of 400 and 5.24 W, respectively, is possible with flexible III-V MJ PV cells. Moreover, the fabrication process of this GaAs-based PV cell comprises the growth of high-quality thin films on reusable GaAs substrates and their transfer to a flexible substrate through epitaxial lift-off (ELO) process[68] which allows the reutilization of the growth substrate multiple times. This reduces the total fabrication cost of flexible PV cells, while overcoming the PCE issue typically associated with other low-cost PV technologies such as a-Si, CdTe or CIGS. Among them, amorphous semiconductor thin films-based PVs have attracted greater attention due to the low fabrication cost and possibility of direct deposition on flexible substrate at reduced temperatures. The mass-production of amorphous semiconductor-based flexible PVs over large areas through roll-to-roll process, makes this technology promising for powering *e*-skin. However, the integration of these materials on stretchable substrates has not been demonstrated so far.

Dye-sensitized PV cells. Dye-sensitized solar cells (DSSC) use a combination of interpenetrating networks based on mesoscopic and wide bandgap semiconductor materials as photo-electrodes with dye-sensitizer electrolytes as light absorbing material electrolytes.[69] DSSCs mainly differ from conventional semiconductor solid-state PV cells in terms of operation which separates the function of light absorption and the carrier charge transportation. This feature can be

Table 1. PV cell efficiency, including PCE and PD reported in the literature

PV technology	PV Material	Substrate	W/g	PCE (%)	PD (W/m^2)	Ref.
Semiconductor solid state: MJ	GaInP/GaAs	Rigid	0.4	46	345	66
Semiconductor solid state: MJ	III-V	Flexible	–	27.6	276	67
DSSC	Redox electrolyte	Rigid	–	11.9	118	73
DSSC	Iodine electrolyte	Rigid	–	11.5	115	72
DSSC+NWs	ZnO NWs	Rigid	–	6.6	66	74
DSSC	TiO_2 NWs	Flexible	–	5.3	53	76
DSSC	TiO_2 NPs	Rigid	–	4.56	46	71
DSSC	ZnO NWs	Flexible	–	3.3	33	75
NFA OPV	NFA polymer	Rigid	–	13.2	133	81
Bulk heterojunction OPV	Polymer	Rigid	–	5–8	49.9	80
OPV	Polymer	Flexible	10	2.5	26	82
Bi-layer OPV	Polymer	Rigid	–	1	6.7	79
QDSSC	Mn^{2+} doping of CdS	Rigid	–	5.42	54.3	86
QDSSC	CdSe + PCPDTBT	Rigid	–	3.2	31.3	87
QDSSC	Cu_2S NPs + CdS/CdSe	Flexible	–	3.08	30.8	88
PSC	Solid-state ionic-liquids + Perovskite	Flexible	–	16.1	150	93
PSC	NC-PEDOT:PSS + Perovskite	Flexible	–	12.32	123.2	65
PSC	Organolead halide perovskites	Flexible	23	12.0	120	35

Characterization carried out using A.M. 1.5 solar simulator (100 mW/cm^2). The table has been organized by PV technologies, being each technology ordered by PCE
PV photovoltaic, *PCE* power conversion efficiency, *PD* power density, *MJ* multi-junction, *DSSC* dye-sensitizer solar cell, *NW* nanowire, *OPV* organic photovoltaic, *NFA* non-fullerene acceptors, *QDSSC* quantum dot sensitized solar cell, *PSC* Perovskite solar cell

advantageous for *e*-skin as in in the case of unstable conditions such as substrate subjected to light or extreme deformations (e.g. bending or stretching of a *e*-skin during the motion of a robot/human) the separation of PV mechanisms could prevent undesirable charge recombination (loss of PCE).

The TiO_2 nanoparticles (NPs) are typically used as photo-anode in DSSCs mainly due to properties such as: (i) anatase crystalline structure for an optimized bandgap; (ii) small particle size to shorten the charge diffusion path; (iii) reduced grain boundaries to limit current resistivity; (iv) significant porosity to enhance integration and interaction between the photon absorbers and the charge-collecting anode.[69] However, a number of alternative hole-transport material (HTM) such as redox mediators and electrolytes have also been investigated, including: (i) I^-/I^{3-} in solid polymer, gel, ionic liquid, or plastic crystal systems; (ii) solid inorganic materials; (iii) Co^{II}/Co^{III} and $SeCN^-/(SeCN)^{3-}$ redox couples; (iv) and hole-conducting organic polymers and small organic molecules.[70] One of the key features that is critical for *e*-skin applications and still need to be investigated is the packaging of DSSCs technology. Potential hazardous/unstable environments and the extreme deformation of the *e*-skin could cause undesired leak of the electrolytes used in DSSCs. For these reasons, the improvement of the packaging would allow DSSCs to be a safe technology to power *e*-skin.

The DSSC based on TiO_2 NPs have the advantage of easy and low-cost fabrication. However, the random distribution of NPs in these DSSCs could increase the disorder in the resulting structure, contribute negatively to trap the charge at the grain boundaries, and therefore, could dramatically compromise the PCE (4.56%) and the output PD (46 W/m^2).[71] This random distribution of NPs can be further fostered by the deformation of the DSSCs during normal operation. For example, during bending of DSSCs powered flexible *e*-skin the distribution of NPs can change and as a result the PCE can be unstable.

Modest gains have been made recently through the development of photosensitizers and electrolytes to enhance the conversion efficiency of DSSCs. For example, the DSSCs based on iodine electrolyte exhibit record values of PCE 11.5% and PD up to 115 W/m^2.[72] The combination of a donor-π-bridge-acceptor Zn porphyrin dye and a tris(bipyridyl)cobalt-(II/III)-based redox electrolyte has been shown to improve the PCE slightly to 11.9% and a PD of around 118 W/m^2.[73] These achievements are promising for powering micro- and nano-devices integrated in an *e*-skin. However, due to aforementioned drawbacks, including potential leakage of the electrolyte and the poor stability of the PV cell performance under deformations, make this technology to be far from its implantation in *e*-skin applications.

Towards the development of flexible DSSCs, metal oxide nanostructures such as ZnO nanowires (NWs) have been demonstrated to improve the resulting structural order of the photo-anode (PCE = 6.6%; PD = 66 W/m^2).[74] Metal oxide NWs with optical fibres or planar waveguides,[75] have been shown to exhibit PCE of 3.3% and PD up to 33 W/m^2. The availability of flexible DSSCs is useful for self-powered *e*-skin, thanks to the new synthesis procedures which is compatible with flexible substrates and drastically reduces the fabrication cost due to the use of earth-abundant materials. For example, well-aligned TiO_2 nanorods arrays grown by low-temperature sputtering technique on flexible substrates have been shown to have PCE of 5.3% and PD up to 53 W/m^2.[76] Alternatively, the progress made in the solution-based methods to synthesize metal oxide nanostructures such as ZnO NWs at low temperatures (100 °C), makes possible the direct growth of these nanostructures on plastic substrates.[77] This has permitted the development of flexible DSSCs at a very low cost and showing stability and without observing cracks of the PV structure under extreme bending conditions (e.g. DSSC cell showing stable performance under 1000 cycles using a 5 mm bending radius[77]).

Organic PV cells. As a result of the growing need to reduce the manufacturing cost of PV cells, organic materials, such as conductive polymers, have emerged as promising candidates.

An essential property of these polymers is the possibility to change their electrical conductivity by conventional doping processes, allowing to create polymers with both donor and acceptor behaviours (i.e. amphoteric properties),[78] and therefore to fabricate a single p–n junction-based PV cell. Organic PVs (OPVs) are mainly based on four different structures, including single-layer, bi-layer heterojunction, bulk heterojunction and diffuse-layer heterojunction.[63] The lowest performance obtained by OPVs is shown by single-layer and bi-layer heterojunction, which present a poor PCE below 1% and maximum PD of 6.7 W/m^2.[79] On the other hand, bulk heterojunction OPV cells exhibit a better performance, showing higher PCE up to 5–8%, and PD of 49.9 W/m^2.[80] The recent advances in the non-fullerene acceptors (NFAs), have further improved PCE to around 13.2% (133 W/m^2)[81] which is closer to the theoretical threshold (15%) estimated for OPV based on fullerene acceptors.

Although the efficiency of the OPVs fabricated on rigid substrates is lower than other technologies, the organic materials are inherently flexible, and this property makes them highly compatible with flexible non-conventional substrates (plastics, fabrics, …). Further they are lightweight and can be realized at low cost of fabrication. These are strong reasons to consider OPV to power *e*-skin.

State-of-art flexible OPVs have successfully demonstrated PCE of 2.5% (and PD of 26 W/m^2) for conjugated polymer/methanofullerene blend.[82] Moreover, comparing the power per mass unit (W/g) of well-stablished PV technologies such as a-Si (0.2 W/g), poly-Si (0.3 W/g), c-Si (0.4 W/g), III-V (0.4 W/g) and CIGS (3 W/g), to ultra-thin OPVs, the latter shows a significant improvement of around two orders of magnitudes (10 W/g).[61] The latter has shown promising performance for the development of energy-autonomous *e*-skin, due to the high PCE above 4%, huge flexibility due to the reduced thickness of 450 nm of the PV structure (2 µm being the substrate thickness), and the reduction of the fabrication cost, replacing ITO by PEDOT:PSS as electrode. In spite of the reduced thickness, this OPV shows an unprecedented mechanical resilience, exhibiting a high device stability under quasi-linear compression to below 70% of their original area, and stability under cyclic compression and stretching to 50%, over more than 20 full cycles. Under these conditions, the OPV presented marginal loss in device performance and no visible defect formation beyond the external contact points. These mechanical properties and compatibility of the materials with human body, make this technology one of the most promising for powering *e*-skin either for robots or as wearable systems for humans.

In addition to the growing PCE of OPVs and their excellent mechanical properties, the semi-transparency of OPVs,[83] rarely observed in other PV technologies such as Perovskite and semiconductor solid-state PVs,[84] has opened a new lines of investigation in smart windows and screens, and therefore, it will be promising for new applications of *e*-skin such as smart windows.

Quantum-dot PV cells. Quantum-dots sensitized solar cells (QDSSCs) have emerged rapidly in the field of PVs mainly due to their unique optoelectronic properties which can be accurately tailored by either varying QDs dimensions or doping processes.[85] Their design which is similar to DSSCs, includes deposition of narrow bandgap semiconductor nanocrystals such as CdSe or CdS, typically on mesoscopic TiO_2 films. Although the photocurrent achieved from QDSSCs is comparable to that of DSSCs, the observed PCE remains low because of the low open circuit and low fill factor. In contrast to DSSCs, the use of I^{3-}/I^--based electrolyte is unsuitable for QDSSCs as it induces corrosion at the working electrode.[86] However, this is not a disadvantage from the point of view of the self-powered *e*-skin, as the absence of electrolyte make this technology suitable for *e*-skin in comparison with DSSCs.

The well-established QDs can have spatially confined charge due to potential barriers and as a result delocalization of the quantum states can take place. This could lead to a multiple-exciton generation (MEG), i.e. each absorbed photon generates multiple electrons, which results in gains above 1 and thus boosts the PCE beyond the above-mentioned Shockley–Queisser limit for Si PV cells. For this reason, QDs based of different materials have attracted a lot of attention during the last years for energy-harvesting technology.

QDSSCs based on semiconductor nanomaterials (e.g. CdSe tetrapods) and low bandgap organic polymers (e.g. PCPDTBT) have been combined to obtained PCE of 3.2% and PD of 31.3 W/m^2.[87] Further improvements have been achieved by doping QDs with metallic impurities (e.g. Mn^{2+} doping of CdS), showing record PCE of 5.42% and PD up to 54.3 W/m^2.[86] This optical doping of active transition metal ions, could modify the electronic and optoelectronic properties of QDs, by creating new electronic states in the mid gap region of the QD, therefore, altering the charge separation and recombination dynamics.

Flexible QDSSCs have been successfully fabricated by depositing Cu_2S NPs on the surface of graphite paper, resulting in a composite counter electrode for CdS/CdSe-based QDSSC. Characterization of this flexible QDSSCs shows PCE of 3.08% and PD up to 30.8 W/m^2, which are promising values but still far from the other PV technologies discussed above.[88] Despite of their poor performance with respect to other state-of-art PV cells, the low weight due to the utilization of NPs, combined with low-temperature processing on non-conventional substrates such as cloth and paper,[88] the QDSSC are excellent for self-powered *e*-skin.

Perovskite PV cells. Organic and inorganic metal perovskite solar cells (PSCs) have emerged as the promising candidates for solar-energy harvesting with excellent PCE and PD.[35,65] The excellent PSCs, combined with features such as flexibility and lightweight, PSCs offer great alternative to current flexible PVs (based on Si, III-V, organic materials, etc.) for *e*-skin applications. As with Si PV technology, the high-temperature procedures conventionally utilized during the manufacturing of PSCs is a major stumbling block in the integration PSCs on flexible substrates. The crystalline quality of perovskite thin films is required for the improved performance and for this reason significant efforts have been put to overcome the temperature bottleneck. These include the transfer of perovskite layers of metal oxide, fullerene derivative and organic materials from growth substrate to foreign flexible substrate.[89–92]

Flexible and small-area PSCs have demonstrated PCE above 16.09%, however, also showing clear cracking of the perovskite layer under bending conditions.[93] Further advances are needed to ensure the mechanical stability and flexural endurance of PSCs towards large-area flexible PVs. In this regard, a promising strategy is to fill the perovskite structure with polymers, preserving the crystallinity of the film, and increasing the reliability of the resulting PSCs over several bending cycles and high bending radii.[65] This approach has shown flexible PSCs with PCE up to 12.32% and PD of 123 W/m^2. Recently, PSCs have demonstrated record values of 23 W/g, with a stabilized PCE of 12%,[35] overcoming performance of photovoltaic technology previously reported in the literature. These PSCs based on chromium oxide–chromium interlayer, which effectively protects the metal top contacts from reactions with the perovskite, have demonstrated great stability for several days under ambient conditions. In addition, the optimized utilization of a transparent polymer electrode treated with dimethylsulphoxide as the bottom layer permitted the deposition from solution at low temperature of pinhole-free perovskite films at high yield on arbitrary substrates, e.g. thin plastic foils with a thickness below

3 µm. Compared to other energy-generating technologies, such as electric generators (0.3–8.4 W/g) and heat engines/heat pumps (0.03–10 W/g for a jet engine, excluding fuel), this PSC technology has a tremendous potential to power wearable and portable devices such as *e*-skin.

While the good performance of flexible PSCs could provide energy surplus for *e*-skin, improved structural stability under deformations make them one of the most promising PV alternatives for self-powered *e*-skin applications.

Mechanical energy

There are a number of ambient mechanical sources of energy (kinetic and potential energies, e.g. in vibrating systems) which can be used to harvest energy to power micro-/nano-devices distributed in the *e*-skin. Mechanical vibrations available in the ambient have wide range of frequencies, from few Hz (human steps, human heartbeat rate, and sea water waves) to several kHz (mechanical engines), and can produce energy in a wide range of few hundreds µWcm^{-3} to mWcm^{-3}.[94] Mechanical energy is helpful to ensure the continuous operation of self-powered systems in circumstances where other energy sources (sunlight, thermal, etc.) are not available. An example of vibration as the source of mechanical energy, in the application unrelated to *e*-skin, can be found in roads and pedestrian paths where cars and humans steps have been used to produce energy.[95] Energy ranging between 50 and 500 µW can be developed in this way.[95] In this regard, there is an intensive research on developing large-area multi-functional mats capable to harvest mechanical energy, e.g. when a car stops in a cross road, allowing also to charge wirelessly its batteries.[96] Another example of a promising on-going investigation has recently demonstrated a prototype of large-area electronic carpet capable to harvest energy from human steps.[97] These technologies are relevant for *e*-skin, as mechanical energy could be harvested by robots or human movements to power the distributed electric components. However, such solutions are often bulky and against the current focus on the micro- and nano-generators to generate energies in the range of nW.

Electromagnetic energy. Using the fundamental principle of electromagnetic induction is another way for obtaining electrical energy to power *e*-skin. For example, a small size (around 0.24 m^3) electromagnetic energy generator, consisting of a magnetic core mounted on the tip of a planar steel beam,[98] could generate up to 0.53 mW (~0.21 mW/cm^3) from vibration having amplitudes and frequencies of 25 µm and 322 Hz, respectively. An alternative architecture successfully used, comprises of a micro-machined generator with a permanent magnet mounted on a laser-micro-machined spring structure next to a PCB coil.[99] This device, occupying a volume of around 1 cm^3, generates 10 µW of power (~0.01 mW/cm^3) using a V_{DC} of 2 V and an input excitation frequency of 64 Hz and amplitude of 100 µm. Significant advances in the micro-/nano-fabrication technology have permitted to achieve better configurations and to reduce the working voltage of the state-of-art electromagnetic-based generators. For example, a micro-generator (~0.1 cm^3) consisting of four magnets integrated on an etched cantilever with a wound coil located within the moving magnetic field has been shown to exhibit output powers of 46 µW (0.46 mW/cm^3) using a V_{AC} of 0.48 V and an input excitation frequency of 64 Hz.[100] The design of such energy harvesters with reduced dimension will improve their integrability along the structure of an *e*-skin. The local energy harvesting is a key feature that will benefit the performance of an *e*-skin. However, the weight of this technology is one of the main drawbacks for *e*-skin. The extremely low dimensions of micro-generators, and more interestingly, the power density generated from excitations in typical ranges of frequencies observed in daily human/robot activities (i.e. walking, eating, driving, etc.), justify them as potential candidates to power an *e*-skin particularly for implantable devices. Nevertheless, in comparison with other technologies discussed in this paper, the electromagnetic-based generators will need further investigations.

Piezoelectrics. Piezoelectricity is based on the electrical energy generation from the deformation of a material. The absence of central symmetry in the crystal structure of a material and the existence of a piezoelectrical potential (or piezopotential) allow the generation of electricity from material deformations.[101] This property has been used to develop passive touch sensors (i.e. sensors requiring no external power for detection of signals) in *e*-skin or in a smartphone screen, where the supply of energy switches on when the sensor is pressed.[102]

Prelaminar piezoelectric energy generator consisted of a thick film piezoelectric material deposited atop a thin steel beam.[99] The bending of the beam produces a deformation of the piezoelectric material, generating an amount of energy up to 3 µW under beam oscillations of 90 Hz. From this pioneer prototype, orders of magnitude improvements have been demonstrated by changing the piezoelectric material. Recently advanced materials and structures, comprising nanostructures and two-dimensional (2D) materials have been explored.[103] Lead zirconate titanate (PZT) has been the most used piezoelectric material for mechanical energy harvesting, showing output power densities up to 416 µW/cm^3 at resonance frequencies of 183.8 Hz.[104] However, the lead content of PZT makes them unusable for several applications. Further, their brittle property can dramatically affect the reliability, durability and safety of this material for long-term operations. A promising alternative for PZT is presented by earth-abundant elements such as metal oxide nanostructures such as ZnO NWs.[103] The biocompatibility, lightweight of NWs, easy fabrication and high performance as result of the crystalline structure of ZnO, make them attractive alternative for *e*-skin applications. Theoretical calculations with clamped-free ZnO NWs (with 50 nm of diameter and 600 nm of length), show it is possible to generate about 0.6 V piezopotential along the NW cross-section when external force is applied at the free end of the NW.[105] This piezopotential is enough to drive metal−semiconductor Schottky diode. In the configuration where NWs are doubly clamped between two electrodes on a flexible substrate, the piezopotential is generated along the *c*-axis of the NW (straining direction), resulting in values in the range of hundreds of volts.[106] The electron screening effect, sometimes observed at the positive side of the NW during the crystal lattice distortion, shows that the intentional/unintentional n-doping of ZnO NWs could hinder the piezopotential.[107] Nonetheless, a reduction of carrier density in ZnO through engineering approaches have made ZnO NWs a promising nanomaterial for self-powered systems.[103]

Strain-induced charge generated by a single piezoelectric ZnO NW, in clamped-free configuration, has been demonstrated by contacting the tip of atomic force microscope (AFM) on the top of NW vertically aligned on the substrate surface.[101] These results exhibit energy discharges of around 0.05 fJ from a single NW, and output powers of 0.5 pW at resonance frequencies of 10 MHz. Considering a NW density of 20 NWs/µm^2, the power density by multiple ZnO NWs vertically aligned on a substrate under similar conditions could be about 10 nanostructures based on sensors.[108,109] Similar experiments have been carried out on different kind of semiconductor NWs, including ZnO (output voltage ~8 mV),[101] CdS (output voltage ~6 mV),[109] InN (output voltage ~1 V)[110] and GaN (output voltage ~0.35 V).[111,112] These works demonstrate sufficient generation of energy required to power nano- and micro-devices with power consumption in the range of µW–mW.[1]

The piezoelectric effect in NWs makes them have higher sensitivity to low-amplitude mechanical vibrations (~Hz), however

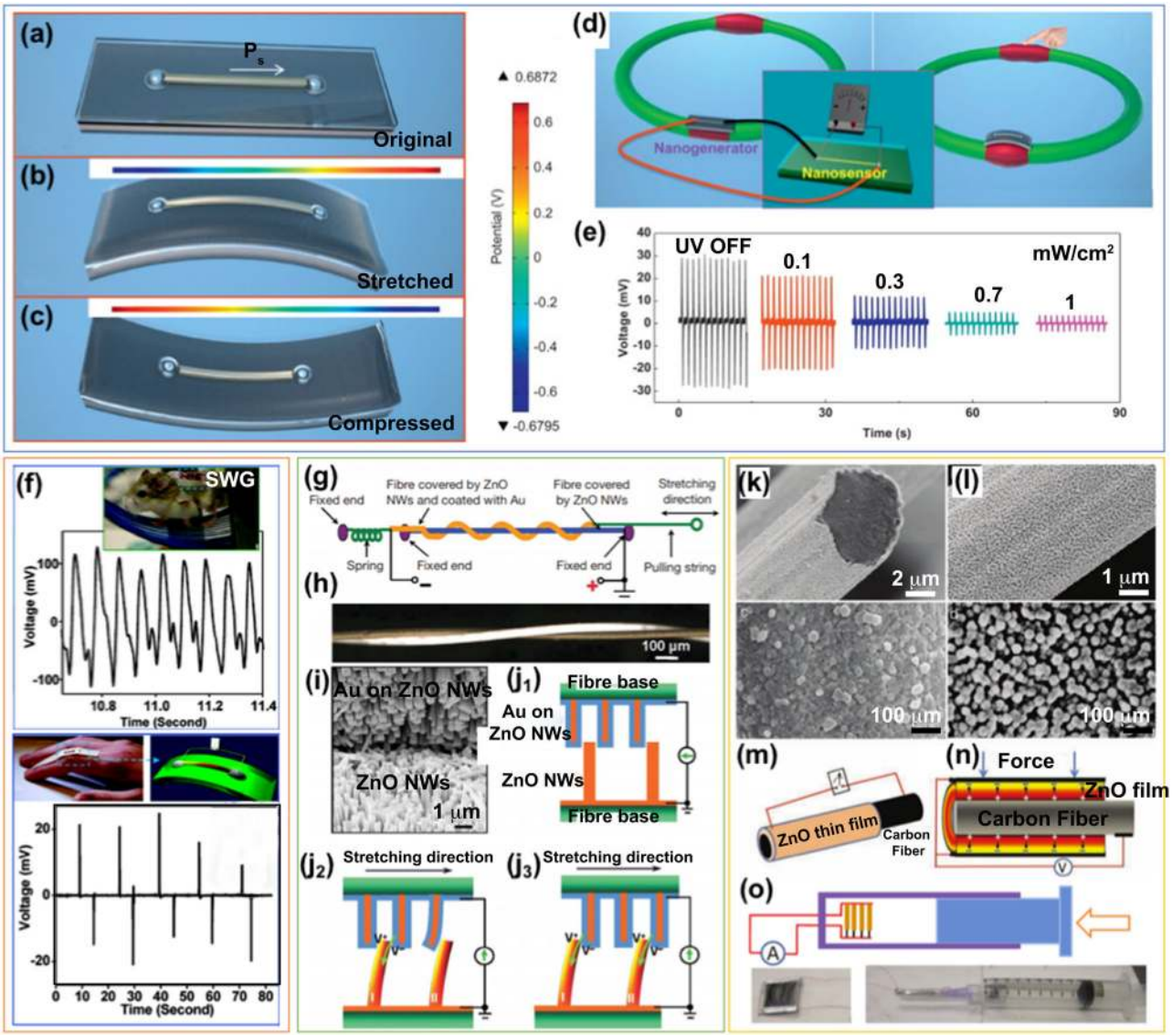

Fig. 3 Piezoelectric energy generators. **a** 3D schema of a single NW-based piezoelectric nanogenerator fabricated on a flexible substrate and subjected to **b** stretching and **c** compression conditions. **d** 3D schema presenting the working principle of a self-powered touch nano-sensors powered by a piezoelectric nanogenerator **a**–**c**. Reprinted with permission from Bai et al.[114] Copyright © 2012 Elsevier Ltd. **f** Energy harvesting from a (top) rat running and (bottom) an oscillating human index finger using a single nanowire-based nanogenerator, namely SWG, including the I–V characteristics. Reprinted with permission from Yang et al.[55] Copyright © 2009, American Chemical Society. **g** 2D schema, **h** optical micrograph and **i** SEM image of a nanogenerator based on fibre-NW heterostructure. $\mathbf{j}_1$–$\mathbf{j}_3$ 2D schema of piezoelectric generation working principle. Reprinted with permission from Qin et al.[119] Copyright © 2008, Springer Nature. **k**, **l** SEM images of ZnO film coating carbon fiber. **m**, **n** 3D Schema of a fiber-based nanogenerator. **o** Schema and pictures of air pressure driven nanogenerator when it is placed inside a syringe. Reprinted with permission from Li et al.[120] Copyright © 2010, John Wiley and Sons

the rectifying, poor contact and the high internal resistance hinder the performance of the NW-based piezoelectric generator and could lower the output down to 2.5 nW/cm^2.[112] This drawback has been recently addressed through different strategies, involving the resonance of single and multi-NW structures. For example, a remarkable improvement (output up to 0.11 μW/cm^2 and a voltage of 62 mV) is observed by paring the metal coated ZnO-nanotip top electrodes with the active ZnO NWs array in a multilayer stack configuration.[113] Such a stacked configuration is well-aligned with 3D *e*-skin applications, with various layers in the stack having different functionalities (Fig. 2). Another approach involves Pt-coated serrated-electrodes as a resonance body to induce a periodic mechanical vibration of vertical-aligned ZnO NWs,[112] and shows output up to 10 μW/cm^2 (10 fW per NW), and output power volume density per NW ranging between 1 and 4 W/cm^3. These values are around 2–3 orders of magnitudes higher than the output from commercial vibrational micro-genrators.[27] The output of these piezoelectric generators can be further improved (e.g. to ~2.7 mW/cm^3 and voltage around 0.243 V) by using doubly clamped configuration, i.e. clamping both sides of the NW (Fig. 3a–c) to transform the output characteristic of the resulting generator from DC to alternating-current (AC) and thus showing a significant increase of the generated power.[103] Thus, the output characteristic of aforementioned ZnO NWs-based piezoelectric generators overcome those issues with conventional PZT for self-powered sensors (Fig. 3d, e),[114] and this make them a promising candidate for the future.

The integration of top-down micro-fabrication procedures together with bottom-up synthesis of semiconductor piezoelectric NWs has demonstrated a remarkable advance with respect to

above approaches. For example, flexible piezoelectric generators fabricated by scalable sweeping-printing have shown power density up to 11 mW/cm^3 and output voltages of around 2.3 V and the generated energy successfully used to power a light-emitting diode (LED).[115] ZnO NWs with a tapered structure (e.g. conical shape, embedded in a polymeric rubber, and sandwiched by two metallic electrodes) can be macroscopic piezoelectric generators (~7000 NWs/mm^2), with output voltage and power of 2 V and 118 nW, respectively, and capable to power continuously a small crystal liquid display.[116] Another approach, also based on AC piezoelectric generators, consists of cyclic stretching/releasing of a single piezoelectric fine wire (PFW) integrated on a flexible substrate.[117] The periodic bending/stretching of the PFW shows record output voltages and energy conversion efficiencies of 50 mV and 6.8%, respectively. The viability of this kind of energy-harvesting devices for low frequencies (0.56 Hz) operation, has been demonstrated for biomechanical energy-harvesting devices for both in vitro and in vivo studies (Fig. 3f).[55,118] In this scenario, the mechanical energy produced by a NW-based nanogenerator attached to either the body of a rat (Fig. 3f, top) or the surface of a human index finger (Fig. 3f, bottom), is demonstrated to be in the range of mV for low-frequency oscillations.

ZnO NWs have also been deposited directly on textile-based carbon fibres—as schematically described in Fig. 3g, experimental probed by optical microscopy (Fig. 3h) and SEM (Fig. 3i)—and used to harvest energy from low-frequency mechanical vibrations/frictions (<10 Hz).[119] The fundamental working principle of this particular configuration is explained in Fig. 3j$_1$–j$_3$. These micro-fibres results in output powers ranging between 20 and 80 mW/m^2, which is attractive for wearable systems as they could harvest energy from expansions/compression by movements in human body such as heartbeat pulses and exhaling actions.[120] In this regard, a relevant example is the carbon fibres coated with ZnO films-based piezoelectric micro-generators (Fig. 3k–n) which create energy from a flux of air pressing their surface (Fig. 3o) and can be used to monitor human health (heartbeat pulses, blood pressure, etc.).[120]

Triboelectrics. Two dielectric materials, when brought in contact, could result in a polarized interface and can lead to generation of electric energy. This could happen either during separating or sliding of dielectric materials (Fig. 4a). This simple mechanism known as tribo-electricity, has remained unknown, ignored, or considered an artefact for years until recently. However, this mechanism is now being explored to transform mechanical energy to electricity to drive a wide range of applications.[46,47,121] A large number of natural systems inherently present motions (e.g. cloth friction during running or walking, engines of a robot under rotation, etc.) and could be active source of triboelectric power for *e*-skin applications.

Triboelectric energy nanogenerators (TENGs) were discovered from "badly" encapsulated ZnO NWs piezoelectric energy generators, where bottom and top electrodes were allowed to slide or contact and the electrostatic induction during the process leading to generation of few volts from triboelectric effect.[37] TENGs are mainly based on low-cost, earth-abundant polymers, which are biocompatible, compatible with flexible substrates, and are environment friendly. These features are key to several e-skin applications (Fig. 4a). Depending on the configuration and material composition, the TENGs could be result from: (i) dielectric-to-dielectric in vertical contact-separation mode,[37] (ii) metal-to-dielectric in vertical contact-separation mode,[44,122] (iii) dielectric-on-dielectric in lateral sliding mode,[123,124] (iv) metal-on-dielectric in lateral sliding mode,[125] (v) rotation mode[126] and (vii) single electrode mode.[127]

The dielectric-to-dielectric in contact mode consists of two polymers brought in contact by an external force with the charge transfer taking place at the contact area (Fig. 4a).[37] This approach has been successfully used to fabricate TENGs with power density of 109 W/m^2 and producing energy from human actions such as shoe sliding or stepping. These TENGs have been shown to drive 600 LEDs (Fig. 4b).[121,122] This approach promising for powering *e*-skin covers such as the feet of a robot or the shoes for humans.

Metal-to-dielectric in contact mode[122] allows development of 3D structures on the same flexible substrate, with multi-layered, small size (14 cm^3), lightweight (7 g) TENGs providing good power (9.8 mW/cm^2 and 10.24 mW/cm^3).[44] The validity of this type of TENGs has been demonstrated by attaching them onto a shoe pad to drive multiple commercial LEDs (Fig. 4c).[44] The dielectric-on-dielectric in lateral sliding mode TENGs show that the in-plane sliding of two dielectric materials can also exhibit triboelectric effect.[123] This approach has been demonstrated to generate power densities up to 5.3 W/m^2, and used to drive hundreds of serially connected (LEDs).[123] Metal-on-dielectric lateral sliding was also been demonstrated using metallic gratings and successfully implemented by stacking up to 10 grating units (3 mm length), producing an output DC current of 0.44 mA (0.18 A/m^2) with an energy conversion efficiency of 8−31% (Fig. 4d–f). This technology was also used to produce an AC output, allowing to light up continuously tens of commercial LED bulbs simultaneously (Fig. 4g).[125] The TENGs based on rotation mode are also based on in-plane charge separation like aforementioned sliding modes, with some additional advantages such as energy harvesting from rotational motions. This feature broadens the range of applications based on centric type motions, and the possibility to adjust the frequency of the rotation which directly has an effect on the TENGs output (Fig. 4h). The disk-based TENG, rotating at 1000 rpm, has been shown to have current densities up to 29.0 mA/m^2 and maximum power densities of 1 W/m^2.[126] While the TENGs presented above are mainly based on two electrodes, the single-electrode-based TENGs have been also demonstrated, which simplifies the engineering design for specific applications.[127] Single-electrode-based TENGs have produced sufficient energy from finger touch actions to drive tens of LEDs. In addition, they have been used as energy source in self-powering tracking system driven by a 4 × 4 matrix of the single-electrode-based TENG array.[127]

Thermal energy

Thermoelectric (TE) materials are a growing area of investigation since the last decade.[128] The possibility to harvest thermal energy, e.g. from heat dissipated by engines (factories, vehicles, robots, etc.) or from heat produced by humans (sport activities, thermo-regulation in inner organs, etc.) and to transform it into electricity would allow to use effectively the energy available in the surrounding environment. The efficient way to scavenge energy without using fossil fuels and non-environmental friendly sources is one of the fundamental pillars for self-powered systems such as *e*-skin. Some examples of thermoelectric energy harvesting for *e*-skin are discussed below.

Bulk and thin film thermoelectric materials. TE generators based on bulk and thin film materials could generate about 0.5 W/cm^3 and 4 mW/cm^3, respectively, at temperature gradients ranging between 20 and 50 K.[129] The TE generators based on bulk and thin film materials have relatively poor efficiency (~10%) and large size, which is not compatible with flexible substrates and hinders their application as energy harvester in wearable systems. Nonetheless, we have included TE generators as potential energy harvesters for *e*-skin, keeping in mind that this technology needs a drastic optimization to match the *e*-skin requirements (flexibility, light-weight, etc.), and the performance demonstrated by the other technologies discussed in the sections 'Light energy' and 'Mechanical energy', as briefly summarized in Fig. 2.

Conventionally, p-type Si-Ge alloys have been used as building

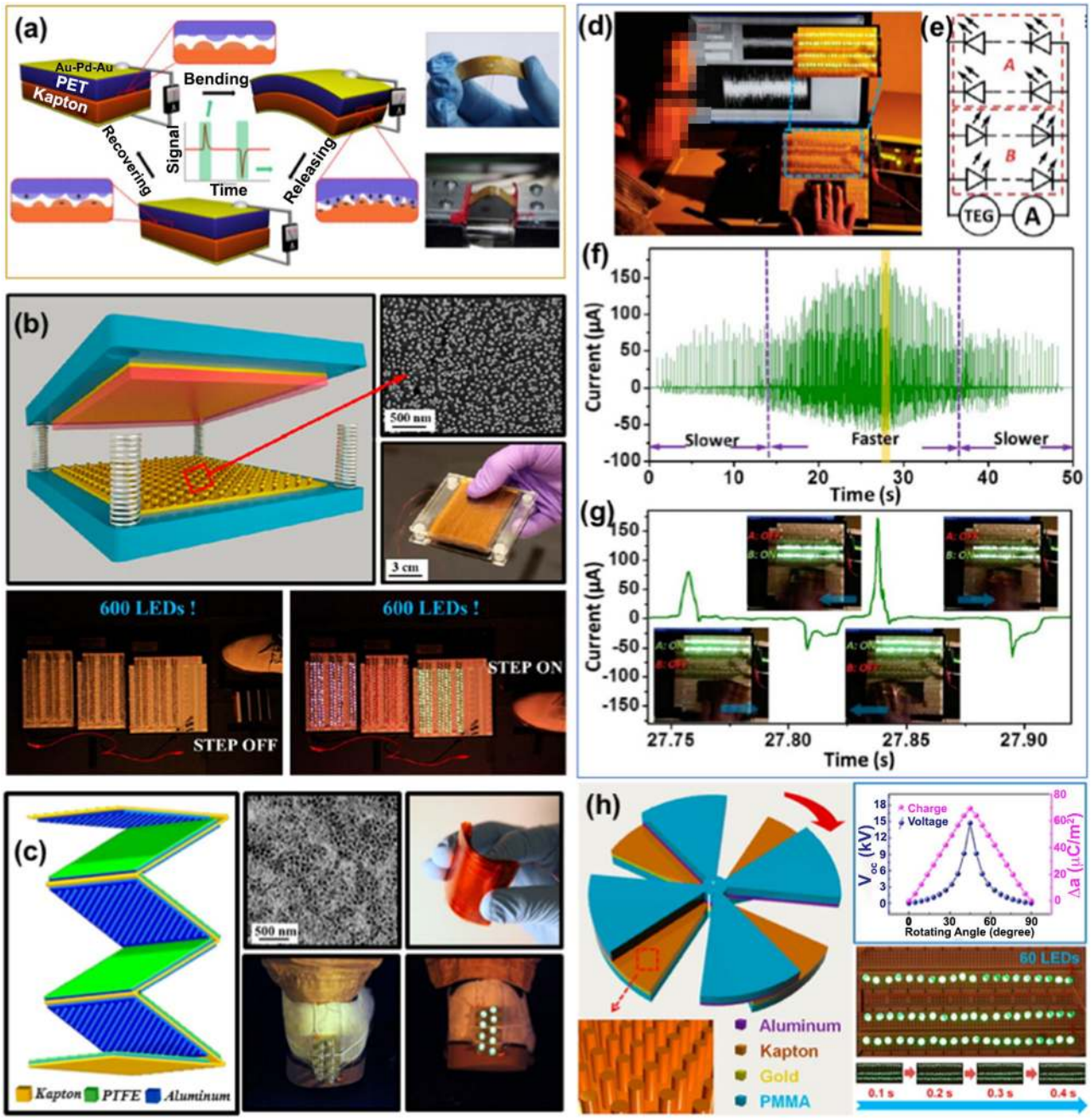

Fig. 4 Triboelectric energy generators. **a** 3D schema (left) and photograph (right) of flexible TEG under bending conditions. Reprinted with permission from Fan et al.[37] Copyright © 2012 Elsevier Ltd. **b** 3D schema, SEM and photograph of TENG (top) and photograph of TENG powering 600 LEDs when footstep falls on the TENG (bottom). Reprinted with permission from Zhu et al.[122] Copyright © 2013, American Chemical Society. **c** 3D schema, SEM and photograph of flexible multi-layered TENG, triggered by press from normal walking. Reprinted with permission from Bai et al.[44] Copyright © 2013, American Chemical Society. **d** Photograph of hundreds of LEDs lighted up by a TENG and **e** electric circuit. **f** Current generated by TENG from a human hand sweeping at different speeds. **g** Current peaks measured at each state of two groups of LEDs during hand sweeping; inset: photographs of the experiment. **h** 3D schema of disk TENG with segmental structure for harvesting rotational energy, electrical characteristics, and demonstration for powering up to 60 LEDs. Reprinted with permission from Wang[46] Copyright © 2013, American Chemical Society

blocks in TE cells, exhibiting *ZT* around 0.5 at elevated temperatures (>900 K).[130] Several new structures and materials have also been explored recently. For example, $Yb_{14}MnSb_{11}$ has revealed a promising increase of both *ZT* (185 μV/K at 1275 K) and Seebeck's coefficient (*S*) (1.0 at 1275 K),[130] the latter having twice the value obtained from Si-Ge alloys. By reducing the thermal conductivity and optimizing carrier concentration in bulk materials, the above approaches have demonstrated high *ZT* of 1.25—at high temperatures around 900 K—and maximum *S* of 200 μV/K.[131] Following this approach, $Ba_8Ga_{16}Ge_{30}$ alloy has been shown to have *ZT* of 1.35 at 900 K, and an extrapolated *ZT* up to 1.63 at 1100 K is predicted, with *S* of 45 and 300 μV/K measured at 300 and 900 K, respectively.[132] Both, p- and n-type semiconductor materials with different structures have been investigated for high-temperature TE applications. The p-type TE materials have shown promising results (e.g. p-type Bi_2Te_3/Sb_2Te_3 superlattices

exhibiting a *ZT* of 2.4 at 300 K and *S* of 243 μV/K) compared to n-type (e.g. n-type $Bi_2Te_3/Bi_2Te_{2.83}Se_{0.17}$ showing a *ZT* below 1.4 at 300 K).[133] Chalcogenide compounds such as $Cs_{1-x}Rb_xBi_4Te$, have also been used as TE materials for near-/mid-room-temperature applications, e.g. showing a *ZT* above 1.5 and a *S* of 100 μV/K at low temperatures around 160 K.[134] Despite excellent advances the performance of above bulk and thin film materials falls short of the requirements for wider nano- and micro-electronic systems.

Low-dimensional thermoelectric materials. From last decades, the significant advances achieved in the synthesis of high-quality nanostructures with excellent control over their properties, as well as the development of highly-controlled integration techniques, have allowed us to use micro- and nano-structures as building blocks in TE generators. For small temperature gradients (i.e. < 20 K), the nanostructures are likely to have better *ZT* compared to their counterpart based on the bulk and thin film materials. This makes them promising candidates as energy harvesters for self-powered wearable systems on flexible substrates.[129,135] The NWs-based superlattices, InSb quantum-dot structures, Si NWs, single wall carbon nanotube (SWCNT) bundle, BiTe NWs and a GaAs NWs, are predicted to have better thermoelectric properties than bulk and thin film materials. For example, *ZT* values greater than 4 and 6 are predicted for 5-nm diameter PbSe/PbS and PbTe/PbSe superlattice NWs at 77 K.[136] Alternatively, tubular nanostructures such as nanotubes (NTs), have also demonstrated a great potential as TE materials. For example Bi_2T_3 NTs have exhibit *S* about 160 μV/K at 300 K,[137] which is higher than those observed in Bi_2Te_3 NWs.[138]

Human body heat energy scavenging. One of the most promising applications of TE micro-/nano-generators is the harvesting of energy from human body heat.[54,139] The human body constantly generates heat from its natural metabolism, which can produces an amount of power around 100 W,[54] and ideal conversion through TE mechanism in to electricity could produce electrical powers of several milliwatts. However, the human body is not a great heat generator, as only a small part that heat energy could be scavenged (about 3–5 mW/cm^2 indoor ambient),[140] and major part is rejected in form of water vapour to the ambient or irradiated as infrared radiation. An *e*-skin with conventional thermopiles (Fig. 5a, left) TEGs or more advanced TE micro-/nano-materials (Fig. 5a, right), covering the human body, could be a futuristic system self-powered by the body heat. For example, if an analog watch (Fig. 5b) or a tactile *e*-skin consume powers in the range of nanowatts,[1] the TE technology can be sufficient. It has been demonstrated that a TE generator placed at the right location on the human body, can produce approximately 10–30 μW/cm^2 of electrical power—in moderate climate—for 24 h. For example, as a practical demonstration of body-powered medical devices, a wireless pulse oximeter based on SpO_2 sensors, successfully fabricated and tested in people (Fig. 5b).[141] This battery-free device used a small supercapacitor (22 mF) as a charge storage element for buffering the radio transmission bursts. In addition, there are some alternative theoretical studies, simulating the temperature difference between core body temperature and the ambient air (Fig. 5c), or modelling the parasitic resistances impacting the TE device performance (Fig. 5d).[41] Additionally, TE generators have been combined with PV cells to obtain wearable devices capable of harvesting energy from ambient light as well as the body heat.[142] For example, a TE energy harvester consisting of many thermocouples connected in series have been used to generate electricity from gradients of temperature observed along the human body, including head (Fig. 5e) and chest (Fig. 5f). This hybrid technology has been validated for self-powered electroencephalography (EEG).[54]

The reduction of the size of thermoelectric generators down to the micro- or even nano-scale is expected to reduce significantly the total weight of the energy harvester, which aligns with the requirements of *e*-skin. For example, Si microwires have been fabricated following the architecture detailed in Fig. 5g, h, exhibiting a strong thermoelectric effect with very low device weight.[36] A maximum of 9.3 mV open-circuit voltage was recorded from the flexible micro thermoelectric generator prototype, with a temperature difference of 54 °C at two ends of the wires (Fig. 5g). The high bendability of this technology allows the development of rolls (Fig. 5g) to increase significantly the compactness and energy output of the resulting device. Similar approaches have been followed to develop other solutions by connecting TE energy generators in series (Fig. 5i, j), forming large-area arrays of generators (Fig. 5k) to increase the overall energy generated by the resulting device.[142] Since this technology is based on micro- and nano-structures the scalability of the process is not expected to hinder significantly the portability (e.g. total weight will still be acceptable) of the resulting technology.

Chemical energy

In addition to thermal and mechanical energies generated by a body (human, animal, robotic, etc.), there is also the chemical energy, which has not attracted much attention so far as potential energy source for powering an *e*-skin. Nonetheless, the recent advances in biofuel cells (BFC) make it possible to harvest energy from human body fluids such as saliva, urine, sweet, blood, etc. through electrochemical mechanisms.[32,143–147] Briefly, the working mechanism of the BFCs is based on biocatalytic redox enzymes reactions to convert chemical energy into electricity. The BFCs are classified based on their biochemical reactions and the nature of the electrodes.[148] The microbial and enzymatic-based BFCs have exhibited record values of performance (micro-BFC: 10–24 μW/cm^2;[32] enzymatic BFC: 32 μW/cm^2).[33] Microbial BFCs use living cells to catalyse the oxidation of the fuel, whereas enzymatic BFCs employ enzymes for this purpose. The advantage of microbial BFCs is that they typically have long lifetimes (up to 5 years). However, microbial BFCs are limited by low-power densities, owing to slow transport across cellular membranes. By contrast, enzymatic BFCs typically possess orders of magnitude higher power densities (although still lower than conventional fuel cells) but can only partially oxidize the fuel and have limited lifetimes (typically 7–10 days) owing to the fragile nature of the enzyme.

Recently, many hybrid approaches have emerged for BFCs, showing better performance with higher power densities up to the range of mW/cm^2, making this technology attractive for powering *e*-skin devices in the future. In most of the aforementioned hybrid technologies, BFCs are based on blood glucose as a fuel, which requires the implantation of the BFCs in the body.[149,150] Nonetheless, non-invasive epidermal BFCs based on temporary transfer tattoos (tBFCs) have been also reported (Fig. 6a) with high power densities ranging from 5 to 70 mW/cm^2.[151] These non-invasive tBFC, tested under different stress and strain during body movement, use lactate as the biofuel particularly during human perspiration when lactate is abundant (Fig. 6b). tBFCs have generated power densities up to μW/cm^2 from cyclic movements (Fig. 6c), demonstrating their applicability to biomedical devices such wearable sweat monitoring sensors.[151] However, for operating the electronics circuits in wearable system much higher power densities are required. In this regard, the advances achieved in printing technologies such as screen printing, have allowed to further improve the performance of BFC electrodes on cloth (Fig. 6a, b).[152] These BFCs fabricated on cloth effectively employ sweat lactate as the biofuel and use it with a customized printed circuit board prototype for the conversion, conditioning and temporary storage of extracted energy (Fig. 6c). In this configuration, the electricity is generated by the oxidation reaction due to sweat lactate at the bioanode and oxygen reduction at the cathode. The cloth BFC generate

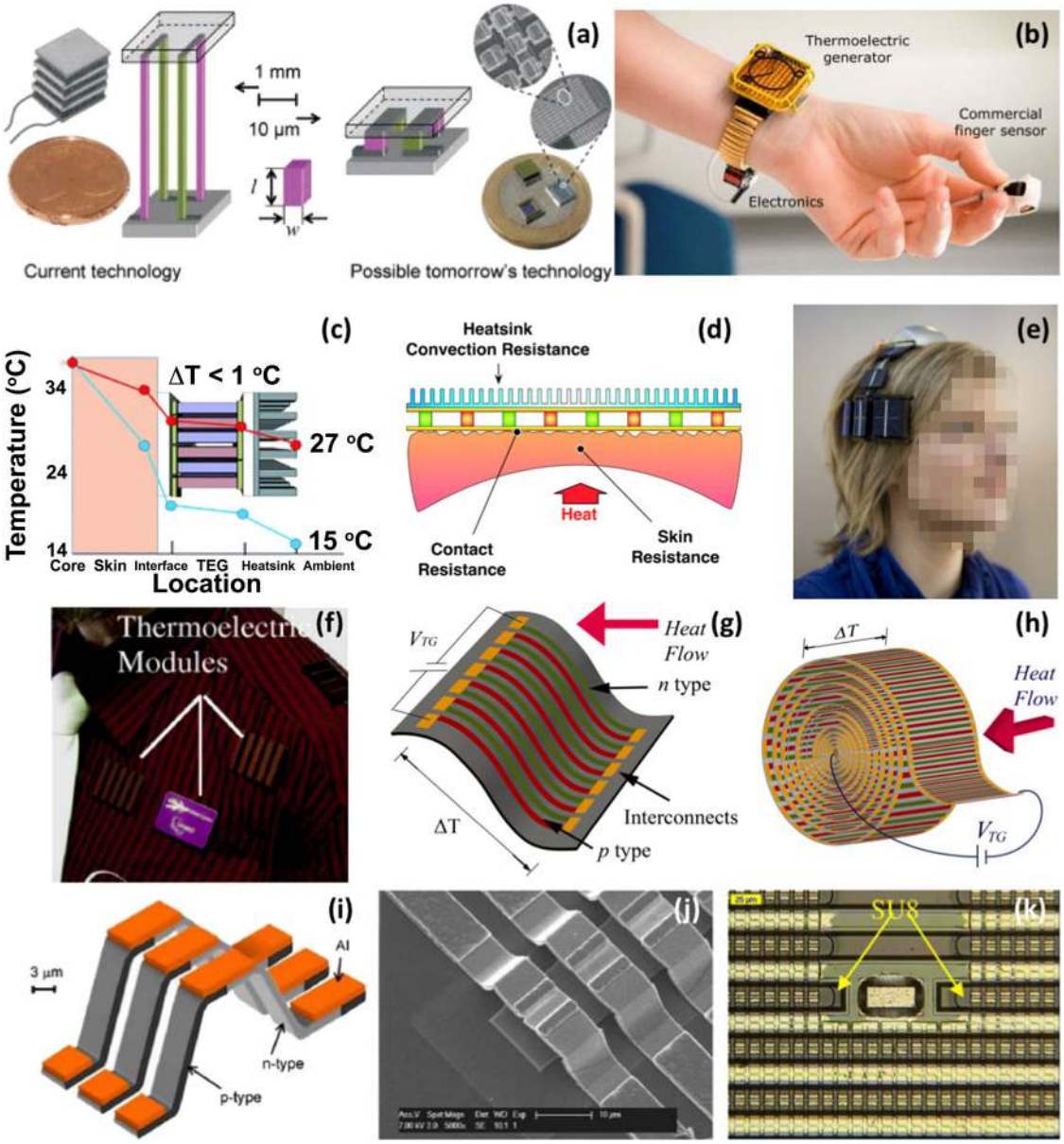

Fig. 5 Thermal energy generators. **a** Current (left) and futuristic (right) view of TE generators. **b** Body-powered wireless pulse oximeter. **c** Temperature difference from core body to the ambient air. **d** 2D schema of parasitic resistances impacting TE performance. Reprinted with permission from Suarez et al.[41] Copyright © 2016, Royal Society of Chemistry. Wearable and wireless energy source-based module, consisting of a thermoelectric energy generator and a PV cell, harvesting energy from human **e** head and **f** body. Reprinted with permission from Leonov et al.[54] Copyright © 2009, AIP Publishing. **g** 3D schema of a flexible TE based on Si microwires with tremendous potential for high compact rolled structures (**h**).[36] **i** 3D schema and **j** SEM image of three thermocouples, and **k** an optical micrograph cross-section, showing their bonding. Reprinted with permission from Su et al.[142] Copyright © 2009, Elsevier

power densities up to 100 mW/cm^2 at 0.34 V during in vitro experimentation and their use has been demonstrated for on-board DC/DC converter and for direct powering of LED or a digital watch.[152] With these recent advances the chemical energy could become a competitive source reaching energy values needed to power nano- and micro-electronic devices distributed in the *e*-skin (as schematically described in the inset of Fig. 6a).

In *e*-skin applications, the use of soft and stretchable electronics is common because it improves the conformability. BFCs have also demonstrated great applicability as they meet such requirements due to their biocompatibility, flexibility/stretchability, and scalability towards high-power-density generation, compatibility to soft substrate to minimize the impact on skin irritation and wearers comfort.[153,154] For such wearable systems, an alternative approach consisting of a layered flexible biofuel based on biobattery with bioanode fabrics for fructose oxidation, hydrogel sheets containing fructose as fuel, and O_2-diffusion biocathode fabrics, has also been reported with maximum power of 0.64 mW at 1.21 V.[155] High energy density and stretchability are the key challenges for this type of biofuels. Highly stretchable textile BFCs have been fabricated by screen printing of stretchable inks with CNT and Ag_2O/Ag electrodes, exhibiting stable power outputs after 100 cycles of 100% stretching.[156] The fabricated BFCs produces power densities of 160 and 250 mW/cm^2 with single-enzyme and membrane-free configurations, respectively, and potential application for self-powered biosensors. In this regard, stretchability feature is currently a matter of intensive investigations in BFCs due to the possibility to complement other

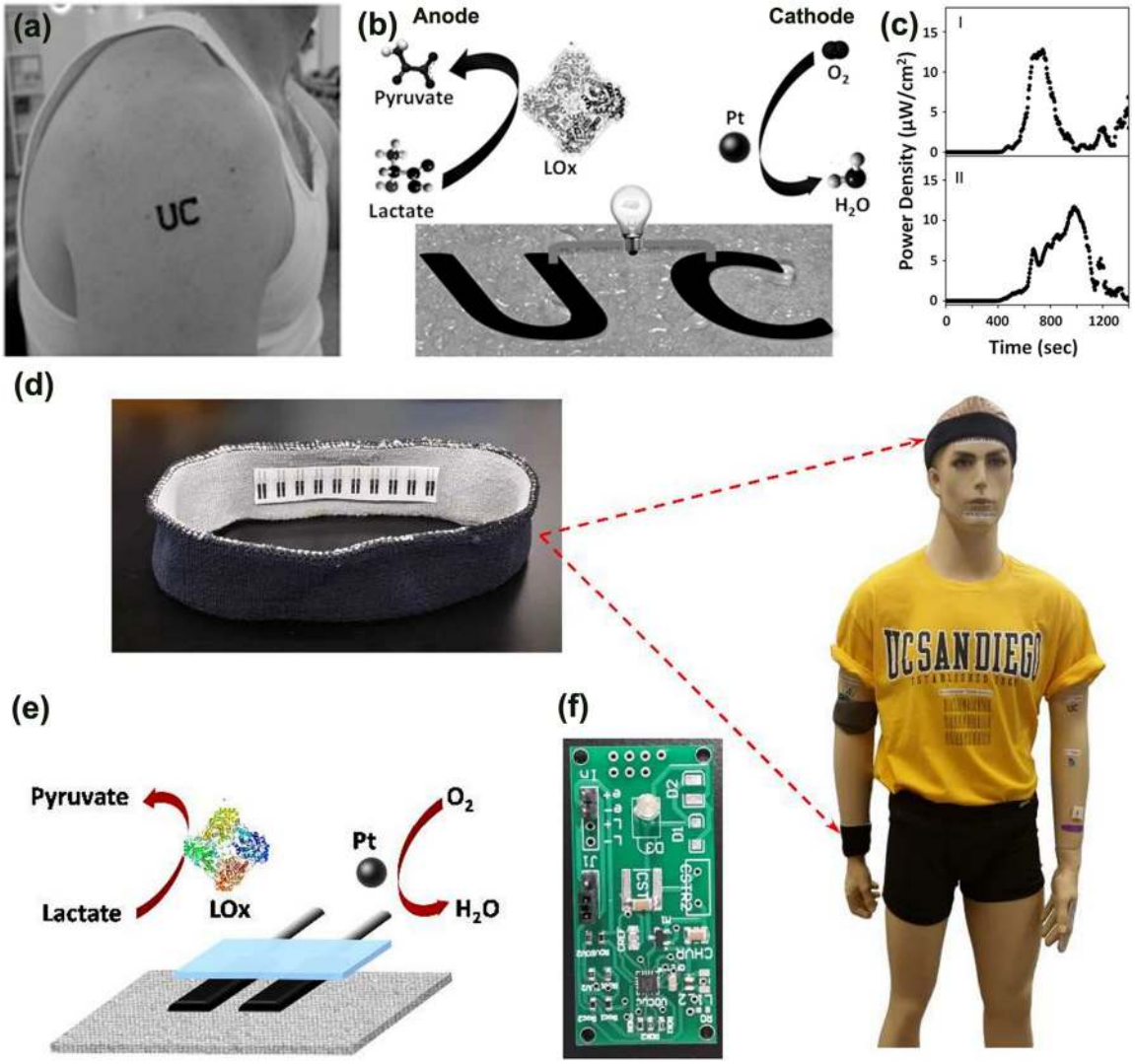

Fig. 6 Chemical energy generators. **a** Photograph of a UC-inspired tBFC integrated on the deltoid of a volunteer. **b** Schematic illustration of epidermal tBFC. **c** Real-time power density profiles obtained during (I) low, and (II) high intensity fitness levels. Reprinted with permission from Jia et al.[151] Copyright © 2009, Elsevier. **d** Photograph of a wearable textile BFCs fabricated on cloth with the shape of a headbands/wristbands; inset: human like dummy wearing the tBFC-based headbands/wristbands. **e** 3D schema of a textile BFC including a bioanode for lactate oxidation and cathode for oxygen reduction. **f** A customized printed circuit board prototype for the conversion, conditioning and temporary storage of extracted energy. Reprinted with permission from Jia et al.[152] Copyright © 2014, Royal Society of Chemistry

technologies such as energy storage devices and sensors currently fabricated on stretchable substrates.

TOWARDS CONTINUOUS ENERGY SUPPLY: TECHNOLOGIES FOR ENERGY STORAGE AND WIRELESS CHARGING

While the efficient harvesting and management of renewable energy sources available in the environment (see the section 'Sources of electrical energy'), are key to the development of self-powered systems (see the section 'Self-powered *e*-skin'), ensuring the continuous supply of energy is also important. To this end, the *e*-skin should also have suitable scheme for energy storage and among various solutions available today the flexible batteries and supercapacitors are the most promising as summarized in Fig. 7a. The integration of both energy harvesting and storage technologies forming a self-powered pack (SPP), is currently an intensive subject of investigation due to its tremendous potential for wearable systems.

One of the main drawbacks of the current portable energy storage technology for *e*-skin and wearable systems is the high dependence on bulky wires for energy transfer, which hinders the portability and autonomy. The wearable systems including sensors for health monitoring electronic patches, and *e*-skin for robots and artificial limbs, require a drastic reduction of wires density (and size), or even the development of a wireless energy transfer technology. Electric vehicles, robots, or artificial limbs are good examples of applications that would strongly benefit by flexible and low-weight energy storage and wireless energy transfer technologies. Some of these are discussed below.

Supercapacitors

Supercapacitors (SCs) have emerged as a promising energy storage alternative to the conventional Li-batteries (LiB), mainly due to properties such as high energy density (17.6 Wh/kg), power density (98 kW/kg), specific capacitance (790 F/g), volumetric capacitance (205.4 F/cm^3), lightweight (10 mg),[157] flexibility

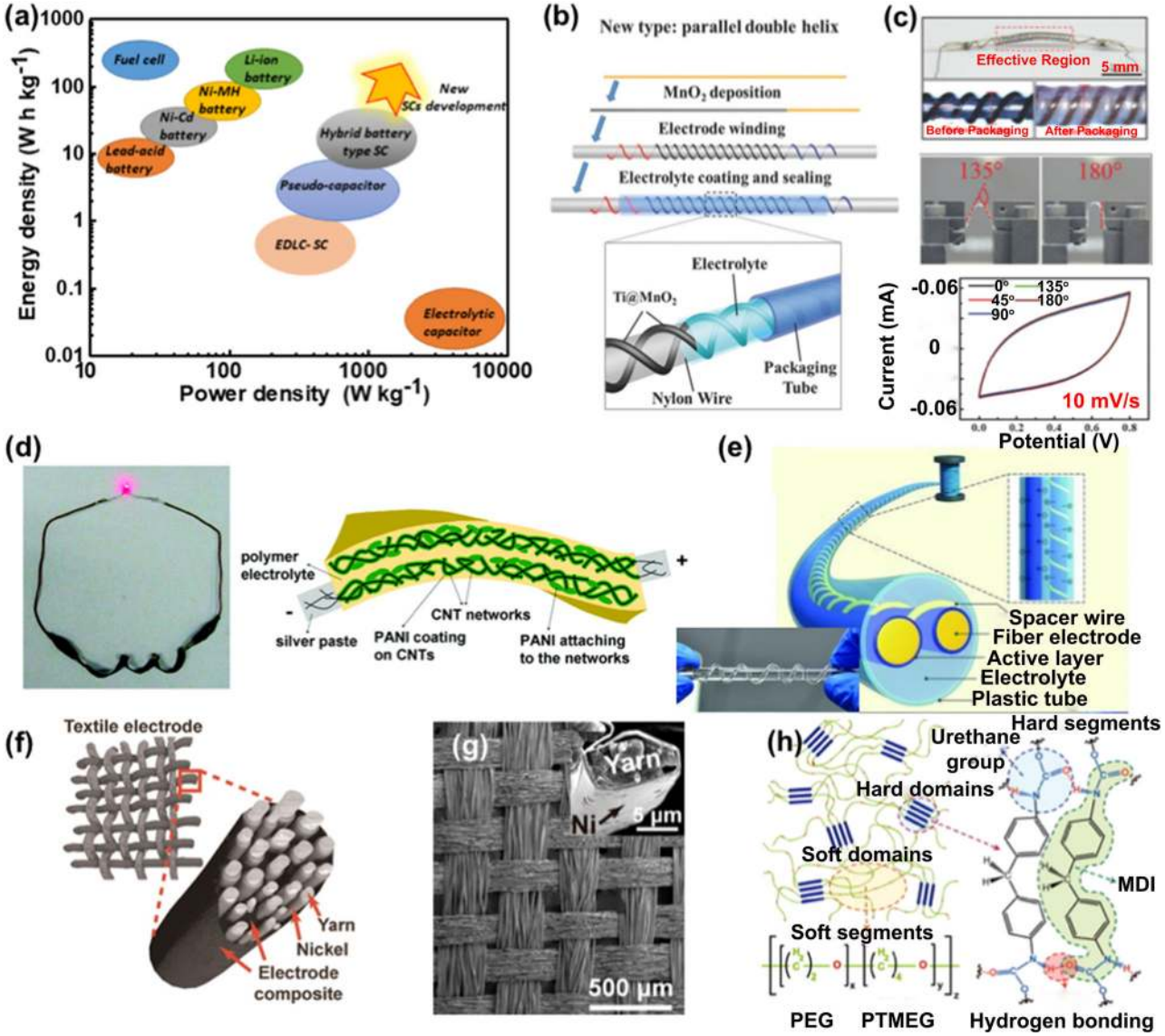

Fig. 7 Energy storage devices. **a** Comparison between batteries and SC technologies performance. **b** 3D schema of wire-shaped SCs. **c** Flexible wire-shaped SC characterized under different bending conditions. Reprinted with permission from Guo et al.[158] Copyright © 2016, John Wiley and Sons. **d** Photograph (left) and 3D schema (right) of CNT-based stretchable SC. Reprinted with permission from Meng et al.[161] Copyright © 2010, American Chemical Society. **e** 3D schema and photograph (inset) of a flexible SC packaged using plastic tube. Reprinted with permission from Fu et al.[164] Copyright © 2012, John Wiley and Sons. **f** 3D schema and **g** SEM image of woven battery electrode yarns, consisting of multiple strands coated by Ni and battery composite. Inset: a cross-sectional SEM image of the Ni-coated textile. **h** 2D schema of the PU molecular structure, highlighting hard and soft domains in PU. Reprinted with permissions from Lee et al.[166] Copyright © 2013, American Chemical Society

(capacitance change <1% under bending angles of 180°) (Fig. 7b, c),[158] cyclic stability (98.3% capacitance retention after 5000 charge/discharge cycles)[159] and stretchability (~30%) (Fig. 7d).[160] State-of-art SCs are generally made of conductive polymers (Fig. 7e),[161] metal oxides nanostructures,[158] carbon-based materials (carbon nanotubes (CNTs) and graphene),[159,160] or hybrid combination of these materials.[157,162] In addition to their excellent energy storage capacity, the SCs are also exceptional because of their quick energy delivery (charging/discharging rates ~50 V/s).[162] This is an attractive feature as in addition to enabling continuous operation of *e*-skin, the SCs could also allow provide energy to operate actuators in artificial limbs in prosthesis and robotics. Further, the fabrication of SCs on non-conventional substrates such as clothes, glove, woven and fabric materials, make them a promising candidate for application such as wearable systems or *e*-skin for fashion industry. In this regard, the fabrication of flexible SCs has been demonstrated by integrating electrochemically active materials such as metal oxides and conducting polymers with flexible fibres made of graphene, carbon, metal and plastic.[163,164]

Wearable batteries

Conventional batteries present drawbacks such as lack of flexibility/stretchability, bulkiness, heavy weight and generation of heat, which have encouraged researchers to investigate alternative energy storage devices such SCs described in previous section. However, due to significantly higher energy density than the state-of-art SCs (e.g. $LiCoO_2$ // Graphite: 387 Wh/kg, R-$Na_2Fe_2(CN)$ // Cu: 336 Wh/kg, $LiMn_2O_4$ // Graphite: 300 Wh/kg),[165] there is still a strong belief that next generation of batteries with flexible and stretchable form factors is possible.

Accordingly, the strategies that are being followed today include using new materials and configurations of the battery components, i.e. current collector, binder and separator, and their role into the mechanical endurance of the battery electrodes, to preserve or enhance the resulting energy storage capacity. For example, a battery consisting of a current collector made of Ni-coated polyester yarn, and binder and separator made of polyurethane (PU) has shown a great enhancement of the electrode mechanical strength, also exhibiting good flexibility (Fig. 7f, g).[166] The PU separator consists of hard and soft domains (Fig. 7h) that prove mechanical strength and flexibility, respectively, to the overall structure of the battery, which are desirable features for its use in the wearable systems. In addition, the PU separators have also demonstrated a significant enhancement of the ionic exchange for the electronic reaction, benefiting the energy storage mechanism. PU also exhibits a superior resistance against thermal shrinkage at high temperatures, which expands further the thermal breakage window of the battery.

The use of CNTs has also been probed for flexible batteries. For example, CNTs-based thin films have been utilized either as current collector with plain paper as a separator (108 mAh/g),[167] or in hybrid electrodes consisting of ultra-long CNTs and V_2O_5 NWs (169 mAh/g),[168] or in $LiMnTiO_4$/MWCNT-based electrodes (161 mAh/g),[169] and in sodium 1,4-dioxonaphthalene-2-sulfonate and MWNTs electrodes (155 mAh/g).[170]

The conventional LiBs do not offer good alternative to above solutions for continuous powering of *e*-skin as, in addition to the mechanical rigidity, they use toxic and/or environment unfriendly electrolytes, which drastically hinder their practical applicability in wearable systems. A common issue observed in LiBs is related to the uncontrolled growth of dendritic Li on the anode surface during the over-charge process, causing the undesired both the short-circuiting of battery electrodes, and the generation of heat. To overcome these drawbacks, more stable materials such as $Li_4Ti_5O_{12}$ (LTO) and $LiMn_2O_4$ (LMO),[171] have been investigated as they exhibit minor volume changes under several charging/discharging cycles. LiBs have also been made from LTO and LMO nanoparticles integrated into two aligned MWCNT yarns, which act as anode and cathode.[171] The fabricated wire-shaped LiBs exhibit energy densities of 27 Wh/kg (17.7 mWh/cm^3), power densities of 880 W/kg (0.56 W/cm^3), and 97% of capacity retention after 1000 bending cycles.

Recently, Zn–air batteries (ZAB) have emerged as a potential environmental friendly alternative of LiBs, mainly due to their high theoretical energy densities (1084 Wh/kg)[172] which are about an order of magnitude higher than LiBs. Flexible fibre-shaped ZAB knitted into clothes and textiles have been successfully reported to exhibit energy densities of around 649 mWh/g.[173] The connection of three fibre-shaped ZABs knitted in series holds a potential of 3.59 V which is sufficient for powering micro- and nano-devices.

Future advances in the *e*-skin will focus on the complex integration of active/passive components such as sensors, actuators, diodes, transistors, integrated circuits on stretchable substrates. In this scenario, the conformability of the *e*-skin constituents will be crucial for their applicability as artificial skin in a wide range of applications. In spite of the extensive efforts to advance stretchable electronics, there is still no great solutions for integrating durable/stable energy storage devices on stretchable substrates. In this regard, the works on dry gel cells based on arrays of batteries embedded in a single elastomer matrix could be interesting direction. These batteries have been demonstrated to withstand stretch ratio up to 100% before failure, delivering open-circuit voltage close to 1.5 V and short-circuit currents up to 30 mA. In addition, these dry gel cells have shown lifetimes above 1000 h and high capacities of 3.5 mAh/cm^2.[174] The experimental process employed to fabricate these cells are compatible with roll-to-roll techniques, which makes this technology promising for the low-cost production of self-powered stretchable systems.

Wireless energy transfer

For future advances in the field of self-powered systems, there is a growing interest on wireless power transfer (WPT) technologies,[175] to allow the wireless charging of energy storage devices and also the wireless use of the stored energy by wearable electronics such as multi-sensing devices in *e*-skin. The magnetic resonate coupling and near-field inductive technologies, also known as near-field communication (NFC), are the two key approaches for WPT.[176] The excellent progress achieved in the field is evident from the WPT-based low-cost and portable modules already available in the market and the growing number of intellectual properties.[177] However, much progress is required, especially to design high energy density devices for implantable applications and for high transfer efficiency.[176] The possibility of charging batteries or SCs through WPT technologies will have tremendous advantage for portable and autonomous systems in a broad number of applications and high commerciality in the market of near-future wearable systems.

Recently, some works have been reported in the area of wireless energy transfer, including SCs directly charged through WPT technologies. For example, nerve simulator applications consisting of a SC with an energy of 860 mJ and a maximum capacitance of 0.2 F, which can be quickly (<2 min) and fully charged through a WPT, and then continuously utilized for 33 h (when connecting micro- and nano-devices loads).[178] Furthermore, a wearable textile antenna has exhibited reasonable good performance in WPT through magnetic resonance mechanism.[179] With four planar spiral coils embroidered with conductive threads, this WPT system could transfer a total power of 12.75 mW with an amplitude of 5.51 dB along a large distance of 15 cm. Nowadays, WPT technology is moving towards the development of high-performance systems with great transfer efficiency and along longer energy transfer distances. In this scenario, much progress will be required in WPT research area, especially in designing architectures (e.g. discovering new materials), high energy density energy storage devices for implantable applications.[180]

Great efforts have been dedicated on the optimization of WPT. Accordingly, NFC technologies has emerged as a promising alternative to achieve the effective transfer of power, e.g. between the energy harvester and energy storage device (charging)[181] or between the energy storage device and the *e*-skin active and passive elements (powering). Both impedance and resonant frequency characteristic of NFC power transfer systems have been investigated to improve the coupling distance resulting in the minor loss of power.[182] As examples of achievements in the field, WPT based on NFC have been successfully utilized in both bio-implantable chips[183] and electric vehicles.[184] These achievements are promising for the self-powered *e*-skin applications covered in this work, where distance between different elements distributed/stacked along the structure of the *e*-skin (sensors, harvesters, storage devices, etc.) are in the typical range of NFC technology.

Wireless powering of sensors is currently an intensive matter of investigation.[31] The current advances related to the design and development of sensors on non-conventional flexible/stretchable substrates, have opened promising alternatives to distribute more number of thin, soft and skin-like sensors along human or robotic body.[185–189] The distribution of these sensors along either robotic or human bodies would a continuous measurement of interactions of robot with the environment (touch sensors, proximity sensors, etc.) or spatiotemporal mapping of physiological health of humans—the latter being relevant for healthcare (electrochemical sensors, temperature sensors, etc.). However, the greater number of skin-like sensors distributed along the body, the more

challenging it becomes to deliver the required power. In order to overcome this challenge, new materials and designs are being studied theoretically and experimentally to reduce the total power consumption of sensors and to allow the wireless delivery of power to acquire sensors data. These investigations have focused on the development of free-battery autonomous multi-sensing *e*-skin (i.e. network of electronic devices sensitive to different stimulus in the environment)[31,190] covering a human body with low-power pressure and temperature sensors (total of 65 sensors distributed along the subject body). The skin is capable of monitoring wirelessly the local pressure and temperature of human subjects sleeping in a hospital bed. Multiple large-scale loop antennas interfaced to radio-frequency (RF) power delivery and data acquisition electronics allow multiplexed operation with a range of tens of centimetres. Output of these sensors were compared with computational modelling, offering a spatiotemporal mapping of physiological processes. Such energy-autonomous sensing *e*-skin could reduce the nursing labour required in a hospital and allow monitoring of multiple patients without the need of expensive beds or complex instrumentation.

SELF-POWERED *E*-SKIN

An *e*-skin consists of multiple sensors (pressure, temperature, chemical, electrochemical, etc.) distributed either along the same surface (Fig. 1a) or stacked as shown in Fig. 1b. With various sensors spread over a large area, mimicking some of the features of human skin, the *e*-skin could bestow robots and prostheses with sense of touch.[1–5] This is particularly relevant for the suitability of robots to carry out delicate tasks, e.g. taking care of elderly, rescue actions in catastrophe zones, high precision operations in space expeditions, etc. The lack of touch or poor sensitivity of current sensing technology used in robots, make the *e*-skin an important matter of investigation. Moreover, the *e*-skin can also act as a 'second skin' in humans,[6] i.e. sticking onto the body surface, with sensors augmenting the natural sensory capacity by measuring various body parameters (e.g. blood pressure, body temperature, heartbeat etc.)[7–13] or ambient parameters (e.g. gases, chemical, materials, radiation, etc.).[14–16] The *e*-skin also require integration of large number of sensing/electronic components on flexible and conformal surfaces,[11,17] as evident from the growing trend of high density of sensors in medical patches,[9,18–24] active-matrix for touch screens[25] and tactile sensitive artificial skins for robots/prosthesis.[1,8] In the particular field of medical care, *e*-skin can be also considered as a potential platform to carry out not only health monitoring (instant diagnosis)[191,192] but also in situ health treatments at specific parts along the human body (controlled self-medication). Moreover, the possibility to coat, e.g. a surgery tool with a *e*-skin would allow the surgeon to get a complete feedback from the patient tissue during the operation.[193]

In this section, we have compiled the most relevant works, reporting the successful integration of both energy harvesting and storing technologies, forming a hybrid system capable to supply continuous energy to power nano- and micro-devices. The main building block of this hybrid technology, named above as SPP, broadens the variety of functionalities of wearable applications such as *e*-skin. This section presents some examples of SPP based on light, mechanical and thermal energies, probing the successful and continuous powering of various wearable applications.

Flexible touch sensors[194] and *e*-skin[1] have been monolithically integrated on a PV cell, resulting in a tactile sensitive system self-powered by sunlight. In 2017, we reported a self-powered transparent, flexible and tactile *e*-skin for a robotic hand.[1] A transparent and flexible *e*-skin was fabricated by integrating single-layer graphene capacitive-based touch sensors (Fig. 8a, b) on top of a flexible and transparent substrate. Resulting touch sensors showing high sensitivity (4.3 kPa^{-1}) to a wide range of pressures (0.11–80 kPa), were coated by a PDMS protective layer, preserving above features over thousands of bending and touching test, as well as, along years of characterization and use (Fig. 8c, d). One of the key features of the fabricated *e*-skin relied on its great transparency, i.e. a sunlight absorption below 5%, which allowed the effective energy harvesting of light energy by a PV cell underneath the *e*-skin (Fig. 8e). The power consumption of the *e*-skin was estimated in the range of mW/m^2. Correlating to the energy produced by the PV technology recorded in Table 1, one can understand that state-of-art PV technology developed in both rigid and flexible substrates, producing energies ranging between 10 and 500 W/m^2, is suitable to power a tactile *e*-skin for robotics and prosthesis applications. In our work, we used a flexible a-Si-based PV cell with an output power density of 192 W/m^2, which is above three orders of magnitudes the energy required to power the graphene tactile *e*-skin. In this scenario, the response obtained from the *e*-skin was successfully used as tactile feedback in an artificial hand (Fig. 8f), allowing the manipulation of rigid and soft objects with different shapes (Fig. 8g).[1] A similar approach followed recently uses touch sensors based on piezo-electronics metal oxide microstructures, self-powered by a perovskite PV cell.[194] Although, the scalability of the approach is not probed so far, the continuous energy autonomy of the touch sensors was demonstrated for periods of time up to 72 h, making the approach promising for future self-powered *e*-skin.

One of the main drawbacks of PV cells in SPPs is that their applicability as continuous energy source for *e*-skin is hindered by periodic absence of sunlight. To overcome this issue, the excess of energy harvested by the PV cell during day time, could be accumulated in the energy storage devices (see the section 'Towards continuous energy supply: technologies for energy storage and wireless charging') for later use, e.g. during night time or poor illumination environments. This will allow in the near-future a fully self-powered *e*-skin for robots and prosthesis using PV technology. Accordingly, the research such as an SPP consisting of a textile-based battery and a flexible solar cell fabricated on a plastic substrate (Fig. 9a–c) is relevant and useful. The energy storage capacity in this case is 13 mAh and a output current density is ~10 mA/cm^2 (at a voltage of 0.4 V, and under simulated AM 1.5G illumination at 100 mW/cm^2).[166] The SPP was used to light up nine LEDs with a power consumption of 42 mW. This type of hybrid technology is useful for *e*-skin where sensors require powers in the range of nW–μW. A similar approach, presenting a SPP consisting of a flexible perovskite-based PV cell and a SC (Fig. 9d), exhibited an effective energy generation which was stored in SC with operational efficiency of 1.15 mWh/cm^3 and a power density of 243 mW/cm^3. The SPP was fabricated on a lightweight fabric woven, benefiting its easy integration in a military uniform for powering wearable devices (Fig. 9e).[56]

The combination of a-Si PV cell and LiB also exhibit a great potential to power high energy consumption devices (~mW).[195] This SPP enabled charging of LiB (up to 4.2 V) using the a-Si PV cell under 1 sun illumination and discharged to 3.6 V at a rate of 20 mA. In addition, the SPP displays energy density of 6.98 mWh/cm^2 and demonstrates capacity retention of 90% at 3C discharge rate and ~99% under 100 charge/discharge cycles and 600 cycles of mechanical bending. The resulting SPP prototype is utilized in different wearable systems, including fashion electronics (Fig. 9f), food quality control (Fig. 9g) and human health monitoring (Fig. 9h, i).

Mechanical energy based on generators such as triboelectric or piezoelectric nanogenerators, namely here TENG[196] and PZNG,[197,198] have also been combined with energy storage technologies forming functional SPPs for different wearable applications. For example, flexible TENGs (Fig. 10a) with capability to generate powers up to around 0.18 $\mu W/cm^2$ from a mechanical source vibrating at 15 Hz were used with SCs based on CF/CNT/RuO_2 electrodes (capacity 87.9 mF/cm^2 at 1 mA/cm^2) and finally

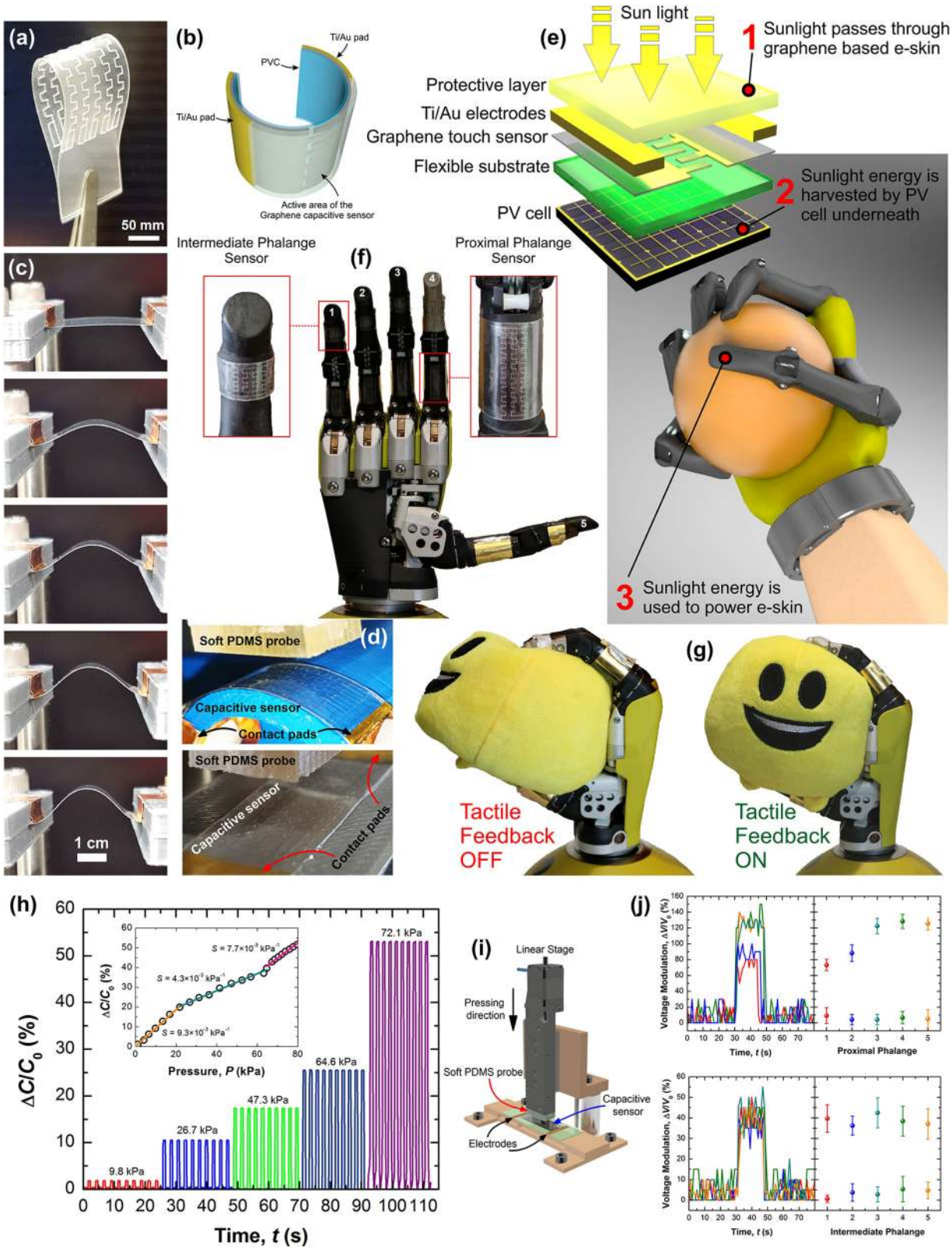

Fig. 8 Touch sensitive *e*-skin powered by light energy. **a** Photograph and **b** 3D schema of a flexible graphene capacitive touch sensor. **c** Dynamic and **d** static bending characterization of sensors. **e** 3D schema of self-powered *e*-skin structure. **f** *e*-skin integrated onto a robotic hand. **g** Self-powered *e*-skin used as tactile feedback for a robotic hand. **h** Touch sensor response vs. applied pressure. **i** Schema of the characterization setup. **j** Response from *e*-skin integrated on a robotic limb (error bars correspond to a series of 10 devices tested up to five times under the same conditions). Reprinted with permission from García Núñez et al.[1] Copyright © 2017, John Wiley and Sons

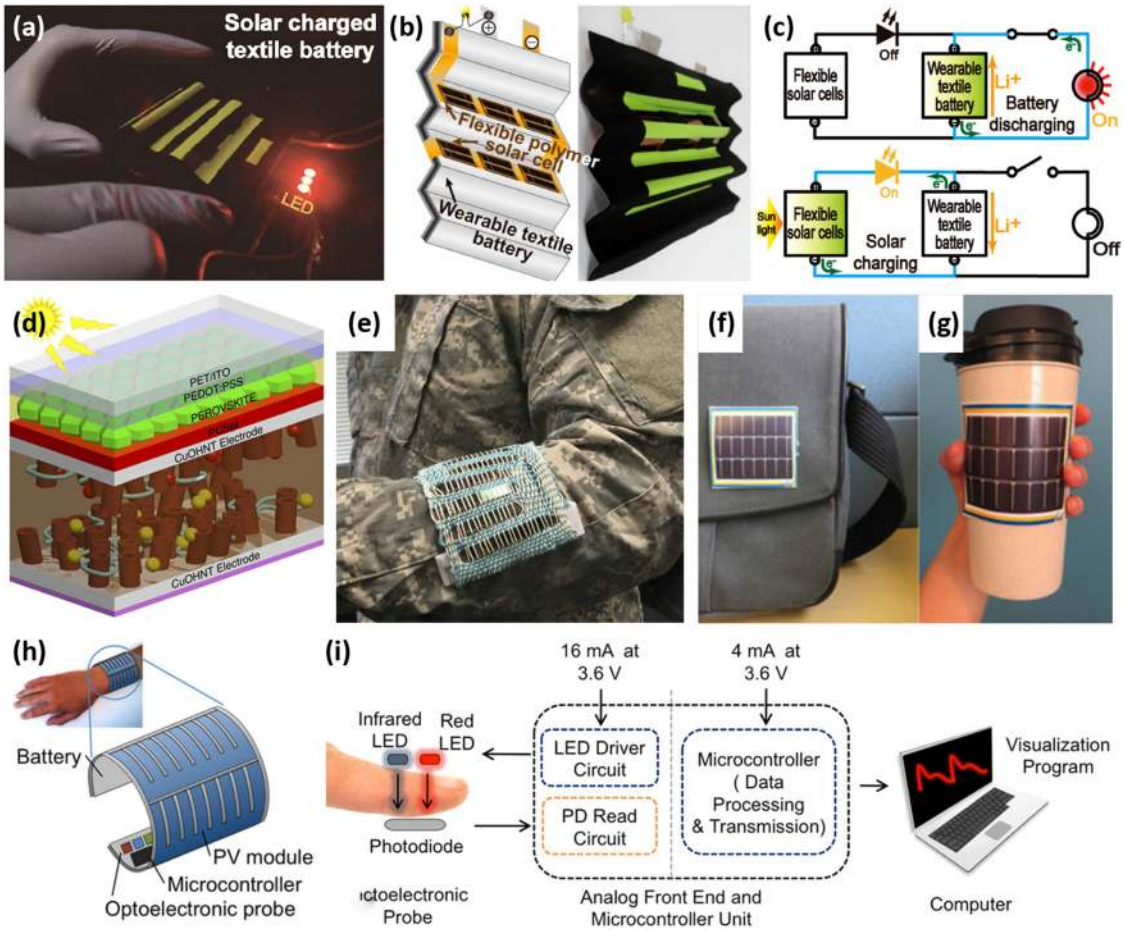

Fig. 9 Self-powered packs (SPP). **a** Photograph and **b** corresponding 3D schema of flexible solar cell and battery integrated forming a flexible SPP. **c** Diagram of SPP working principle. Reprinted with permissions from Lee et al.[166] Copyright © 2013, American Chemical Society. **d** 3D schema of a SPP consisting of a perovskite PV cell and a SC. **e** Photograph showing a military uniform incorporating a lightweight fabric woven SPP and cotton threads. Reprinted with permission from Li et al.[56] Copyright © 2016, Springer Nature. Photographs of a flexible SPP consisting of a flexible PV cell and a LiB wrapped on a **f** bag and **g** a travel mug. **h** 3D schema and **i** working principle of a pulse oximeter powered by a SPP. Reprinted with permission from Ostfeld et al.[195] Copyright © 2016, Springer Nature

utilized to light up an LED (Fig. 10b).[196] The developed unit called self-charging micro-supercapacitor power unit (SCMPU) was inserted in the insole of a shoe, allowing to light up continuously LED during a daily human walking (Fig. 10c). Moreover, TENG and SC-based SPPs have been fabricated on a conductive carbon fabric to improve the wearability.[199] The TENG generated 33 V and 0.25 μA at a frequency of 1.5 Hz, producing a power of around 0.18 $\mu W/cm^2$, which was stored in a SC based on CF/CNT/RuO_2 electrode with a capacity of 87.9 mF/cm^2 at 1 mA/cm^2 (Fig. 10d, top). The frequency of various human actions (i.e. walking, running, stretching, etc.) was demonstrated to produce different charge accumulations in the SPP, i.e. these actions produced electricity exhibiting a proportional relationship within a speed of motion (Fig. 10d, bottom). This interesting feature allows the device to function as a wearable self-powered human activity monitor (Fig. 10e). With suitable material structure, design and fabrication processes on electrostatic generation, the performance of storage and its application can be further improved.

In case of PZNGs, different approaches, including materials and structures, have been studied for SPP. For example, CuO/PVDF-based nano-array piezo-electrodes have demonstrated the generation of a great internal piezo-electrochemical potential, which was combined with a LiB to result in a SPP.[197] The resulting SPP presented a storing capacity of 0.0247 μAh and an energy capacity of 6.12 μJ, by means of applying a force around 18 N with a frequency of 1 Hz.

Furthermore, SC and PZNG have been successfully combined in a SPP,[198] which consists a self-powered electrokinetic SC for mechanical-to-electrical energy conversion. Here, the SC was made with a CNT-coated Ti-mesh active electrodes and anodic aluminium oxide (AAO) nano-channels as a separator membrane (Fig. 10f). The characterization of the SPP showed that under pressure of about 2.5 bar, through the electrokinetic effect in AAO nano-channels, a charge density up to 0.4 mC/cm^2 was stored in the SC. These SPPs presented high scalability as demonstrated by the effective fabrication of a prototype consisting of a 3×3 integrated system, in which the device and electrolyte are sealed in an organic glass tube by two movable rubber plugs (Fig. 10g). The integrated devices exhibited an electrochemical potential window of 3.6 V and a great capacitive performance (Fig. 4b). In addition, the use of an 8 kg load on top of the SPP, fully charged the SC of the SPP within 5 min, being 40 μJ the maximum energy released charged from the SPP during the discharging of that SC.

KEY CHALLENGES AND POTENTIAL SOLUTIONS FOR FUTURE SELF-POWERED *E*-SKIN

It is clear from discussion in previous sections that the *e*-skin could strongly benefit from the latest advances in the field of energy

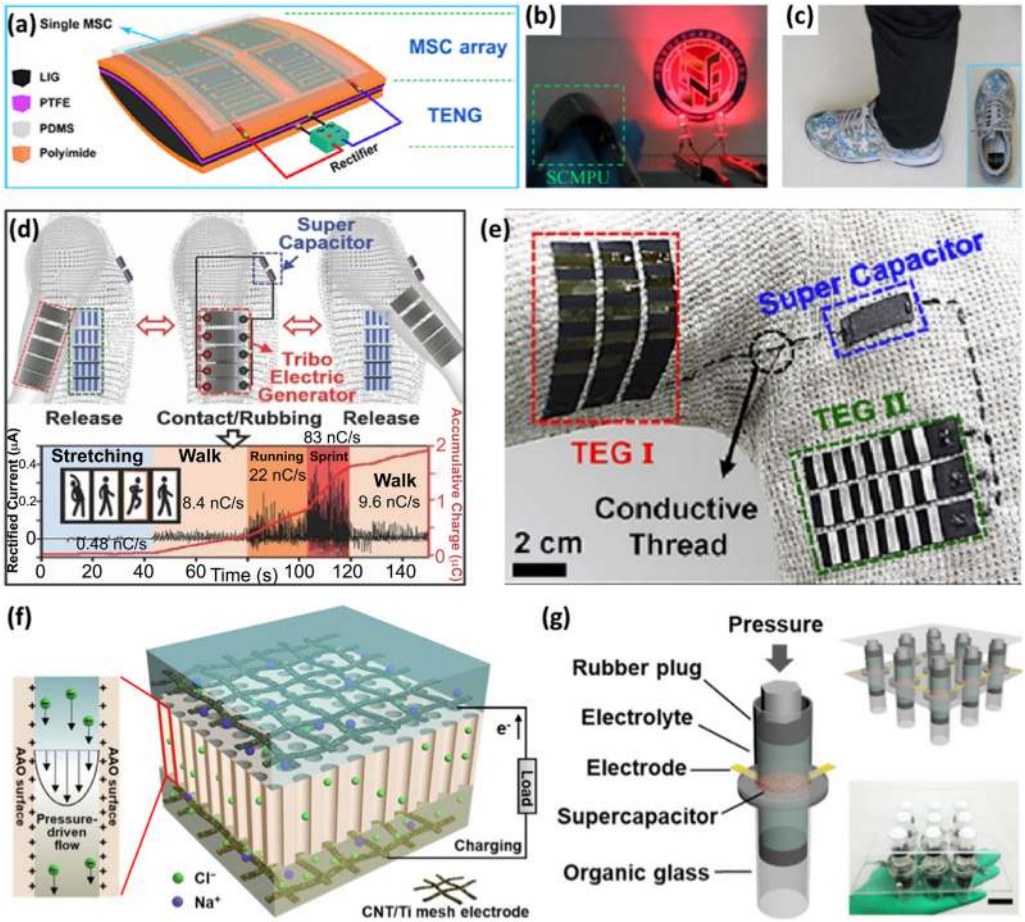

Fig. 10 Self-powered wearable *e*-skin: self-charging devices. **a** 3D schema of flexible SCMPU. Photograph of **b** bent SCMPU generating enough power to light up LEDs, and **c** SCMPU inserted in the insole of a shoe. Reprinted with permission from Luo et al.[196] Copyright © 2015, Springer Nature. **d** Schema showing the charging/discharging mechanism of SC by TENG (top) and SC output under different human activities (bottom). **e** Photograph of SPP manufactured on fabric, consisting of TENG and SC and integrated on a jersey. Reprinted with permission from Jung et al.[199] Copyright © 2014, John Wiley and Sons. 3D schema of **f** a single SPP consisting of CNT/Ti electrode and AAO membrane as SC, and PZNG, and **g** a 3 × 3 array of SPP connected in series. Reprinted with permission from Yang et al.[198] Copyright © 2018, American Chemical Society

(e.g. stretchable PV cells,[28] high capacity supercapacitors,[30] wireless power transfer,[180] etc.). Several challenges need to be overcome to realise the full potential offered by these advances and to obtain a high-performance energy-autonomous *e*-skin. These relate to: (i) tailoring mechanical properties,[6,10] (ii) integration of various technologies resulting in a hybrid system,[166,170] (iii) device architecture[200] and packaging,[1] (iv) efficiency and capacity of energy storage technology,[30] (v) low-power electronics to ensure positive energy budget,[8,201] (vi) lightweight and cost,[30,166] (vii) new compatible ways to harvest energy,[122] or new sources available in the environment,[44,202] and (viii) the secure transmission of sensor data and energy through wireless protocols (IoT).[203]

The next generation of *e*-skin pursues the development of micro- and nano-sensors and electronics on soft and polymeric materials to improve the mechanical properties such as stretchability and lightweight. This technology is known as soft-robotics,[57,204] and comprises 3D printing of artificial limbs with *e*-skin covering/embedded along its surface, and for this reason is nowadays considered one of the most promising lines of investigation.

The integration of different technologies, i.e. compatibility of hybrid systems, is still a matter of intensive investigation. Different thermal expansion coefficient, or chemical stabilities under different processing environments, are some of the hurdles in the way of achieving hybrid integration in *e*-skin. These drawbacks could be overcome with materials presenting multi-functionalities. For example, graphene has been used as electronic layer, temperature sensor and pressure sensor, all integrated on the same flexible substrate, reducing the incompatibility of each functional layer.[205]

The fabrication of next generation of *e*-skin involves the design of new architectures to ensure an reliable interaction using *e*-skin, e.g. a robot wearing a *e*-skin grabbing and moving an object.[1] Once the 2D technology reaches the limit of minimum device size and device-to-device distance, the 3D stacking of multi-functional layers is expected to be the next generation of *e*-skin and wearable systems[57,206] to add more components and to use material properties such as optical transparency or semi-transparency.

Several works on *e*-skin[50] have focused on increasing the device density per unit area by reducing the size of the electronic components (sensors, transistors, diodes, etc.) and developing new approaches to improve their integration over large-areas.[39,188,207,208] In the initial phase of *e*-skin development the use of low-power electronics was a matter of intensive investigation. However, nowadays the research revolves around new energy sources and energy harvesting and storage strategies to power already existing low-power micro/nano-devices (sensors, transistors, diodes, etc.) to realise a self-powered *e*-skin.

Conventional energy harvesting (PV cells, thermoelectric energy generators, piezoelectric energy generators, etc.) and storage technologies (Li-ion batteries) are incompatible with non-conventional flexible/stretchable substrates. Although some progress has been made in this direction (e.g. flexible organic PV cells,[209] PV cells integrated on cloths,[64] stretchable PV cells,[28] nanogenerators capable to harvest mechanical energy,[44,124,202] or high capacity flexible supercapacitors[30,161,164]) further investigations will be needed in terms of features such as lightweight, low cost, biocompatibility, low-toxicity, durability and stability in hazardous environments. The compatibility of these latest technologies with each other will be crucial for realising hybrid energy systems to exploit two or more harvesting mechanisms simultaneously. For example, stacking of graphene-based transparent *e*-skin on top of a flexible PV cell requires the compatibility in terms of process parameters, and fabrication steps etc. Likewise, integration of sensors on textile-based stretchable PV cells will be advantageous for wearable self-powered applications. In the field of PV cells, the most promising approaches that are being explored are PV cells based on quantum dots[210] and perovskite materials.[65,89] With respect to the technologies based on mechanical energy harvesting, tribo-electricity has opened new lines of investigation offering higher efficiencies than those obtained by conventional piezoelectric generators.[44,45,122] In this regard, triboelectric generators have demonstrated the potential to harvest that energy that was wasted (wind, water, human body motions, etc.).[121,127]

The tremendous advances achieved in nano-fabrication technologies allows nowadays to expect a significant reduction in the size of components (e.g. energy harvesters,[210] energy storage devices[30] and electronic components[8]) that are needed in the *e*-skin. The integration of these components over large areas is challenging especially due to materials have different fabrication processing requirements. Often thermal budget issue hinders the direct integration of these components on flexible substrates. Further, compared to the conventional technology developed on Si wafers, the high surface roughness and porosity of flexible and stretchable substrates typically used in *e*-skin applications,[5,6,16,50,57,211] hinder the improvement of the component density per unit area. In this regard, there is a growing research on assembly techniques that allow effective transferring and positioning of micro- and nano-components (sensors, capacitors, transistors, lasers) at specific places along a receiver substrate.[14,36,212–215] This approach is promising because it prevents the direct synthesis of high crystal quality materials on flexible/stretchable substrates, which is one of the main limitations of this kind of non-conventional materials.

In the particular case of wearable systems, biocompatibility will require further investigations. Currently, majority of the high energy density SCs are based on environment unfriendly materials. Nanostructured materials used in stretchable or flexible SCs cause several challenges such as low life cycle, lack of stability in high current densities, low energy density, etc. Engineering in activated carbon-biocompatible metal oxide composite with high electro active surface area, ion exchange conductivity and high hydrophilicity will further enhance the energy storage performance of future SCs. The development of such systems in textile or fibre-based substrate will be advantage for the wearable system. In addition to this, the majority of hybrid self-powered systems have energy storage and generators as two separate components. Further advances are required to develop in-built energy storage and generators on single devices.

Another important area of investigation that will foster the rapid evolution of future *e*-skin is the wireless power transmission (WPT) technology. WPT is expected to create a huge impact on both, conventional Li-ion batteries and SCs, allowing the charging of above energy storage technologies while preventing the utilization of any bulky wire and complex interfaces. WPT is currently being investigated in fields such as medicine (biomedical implants[176]) and automation (e.g. Faraday institute for replacing fuel by batteries in UK vehicles[216]) where the wireless charging of batteries (or future SCs) will be a breakthrough achievement compare to the current state-of-the-art technology. WPT has also attracted significant attention in the field of wearable self-powered systems, and particularly in *e*-skin applications, where some preliminary results have demonstrated promising results.[217] However, drawbacks such as low distance range of the energy transfer, screening effects in the environment, or slow charging rates, make WPT still a technology that requires further investigations.

Near-future *e*-skin will need the hybrid integration of above technologies, e.g. by combining PV and tactile sensors,[1] powering pH sensors by a portable energy pack consisting of a PV cell and a SC,[9,30] or integrating thermoelectric generators to harvest thermal energy from a human body and to power multi-sensors distributed along an *e*-skin.[54] These are representative examples where the integration of different technologies has not been possible so far due to several reasons including non-compatibility because of the toxicity/reactions of different materials, substrate constraints, fabrication temperature limits, mechanical stress under bending conditions, etc. In this regard, integration technologies and specially 3D integrated circuit (IC) approach, comprising layer-by-layer printing,[7,212,218] flip-chip bonding, roll-to-roll (R2R) printing[215,219] could offer the solutions.

DISCUSSION

This review analyses the most promising energy harvesting and storage technologies to highlight the development of a compact energy system for energy-autonomous *e*-skin. The in-depth discussion on various energy sources (e.g. sunlight, mechanical, thermal, and chemical) and storage methods (batteries, supercapacitors, etc.), as well as, energy transfer through wireless technologies, highlights suitable options for continuous operation of multiple electronic devices and sensors distributed along the *e*-skin. As explained in this review, the use of hybrid energy systems made from the combination of two or more energy-harvesting mechanisms, will result in a new advanced technology capable to work continuously with stability, even during the short absence of some of energy sources.

Advanced new materials and structures leading to higher power conversion efficiencies from light, mechanical, thermal, and chemical energy sources to electricity, are likely to appear next, which will allow reduction of cost, size and weight of next generation of energy harvesters. In this scenario, both organic and inorganic materials with the shape of nanostructures are promising candidates for the development of near-future PVs, piezoelectronics, triboelectronics, thermoelectric generators, etc. Some of the above energy-harvesting technologies, which were covered in this review, have already reached the market, and have been successfully developed on flexible/stretchable and light-weight substrates.[28,37,41,102] This new technology will offer an excellent opportunity for the development of self-powered systems, e.g. for *e*-skin, wearable patches, smart-devices, etc. for different applications (robotics, human health monitoring, environmental monitoring, etc.). Apart from above energy sources, tremendous potential lies in the field of biofuels to power *e*-skin used for human health monitoring.

These new technologies combined with a rapid development in the field of energy storage devices such as supercapacitors or ultracapacitors combined with progresses in the field of wireless energy transmission, will produce a significant growth in the field of self-powered systems. Especially for *e*-skin applications, where the energy requirements of distributed sensing/electronic components are in the range of hundreds of nanowatts. Finally, the integration of energy systems (i.e. harvester, storage, and

transmitter) with *e*-skin will allow continuous powering of various components, thus improving the user acceptability of this interesting technology.

DATA AVAILABILITY

All data are available within the article or available from the authors upon reasonable request.

ACKNOWLEDGEMENTS

This work was supported by the EPSRC Engineering Fellowship for Growth – PRINTSKIN (EP/M002527/1) and neuPRINTSKIN (EP/R029644/1).

AUTHOR CONTRIBUTIONS

C.G.N. and R.D. conceptualized the work; C.G.N., L.M. and R.D. collected the data and contributed to the scientific discussions and wrote the manuscript. R.D. provided overall supervision of the work.

ADDITIONAL INFORMATION

Competing interests: The authors declare no competing interests.

Publisher's note: Springer Nature remains neutral with regard to jurisdictional claims in published maps and institutional affiliations.

REFERENCES

1. García Núñez, C., Navaraj, W. T., Polat, E. O. & Dahiya, R. Energy-autonomous, flexible, and transparent tactile skin. *Adv. Funct. Mater.* **27**, 1606287 (2017).
2. Tee, B. C., Wang, C., Allen, R. & Bao, Z. An electrically and mechanically self-healing composite with pressure-and flexion-sensitive properties for electronic skin applications. *Nat. Nanotech.* **7**, 825–832 (2012).
3. Bauer, S. Flexible electronics: sophisticated skin. *Nat. Mater.* **12**, 871–872 (2013).
4. Wang, C. et al. User-interactive electronic skin for instantaneous pressure visualization. *Nat. Mater.* **12**, 899–904 (2013).
5. Yogeswaran, N. et al. New materials and advances in making electronic skin for interactive robots. *Adv. Robot.* **29**, 1359–1373 (2015).
6. Benight, S. J., Wang, C., Tok, J. B. & Bao, Z. Stretchable and self-healing polymers and devices for electronic skin. *Prog. Polym. Sci.* **38**, 1961–1977 (2013).
7. Takei, K. et al. Nanowire active-matrix circuitry for low-voltage macroscale artificial skin. *Nat. Mater.* **9**, 821–826 (2010).
8. Navaraj, W. T. et al. Nanowire FET based neural element for robotic tactile sensing skin. *Front. Neurosci.* **11**, 1–20 (2017).
9. Dang, W. Stretchable wireless system for sweat pH monitoring. *Biosens. Bioelectron.* **107**, 192–202 (2018).
10. Dang, W., Vinciguerra, V., Lorenzelli, L. & Dahiya, R. Printable stretchable interconnects. *Flex. Print. Electron.* **2**, 013003 (2017).
11. Gupta, S., Navaraj, W. T., Lorenzelli, L. & Dahiya, R. Ultra-thin chips for high-performance flexible electronics. *NPJ Flex. Electron.* **2**, 1–17 (2018).
12. Kim, J. et al. Wearable smart sensor systems integrated on soft contact lenses for wireless ocular diagnostics. *Nat. Commun.* **8**, 14997 (2017).
13. Manjakkal, L., Sakthivel, B., Gopalakrishnan, N. & Dahiya, R. Printed flexible electrochemical pH sensors based on CuO nanorods. *Sens. Actuator B-Chem.* **263**, 50–58 (2018).
14. García Núñez, C., Liu, F., Xu, S. & Dahiya, R. *Integration Techniques for Micro/Nanostructures Based Large-area Electronics*, *Cambridge Elements* (Cambridge University Press, Cambridge, 2018).
15. Wang, T. et al. Flexible transparent electronic gas sensors. *Small* **12**, 3748–3756 (2016).
16. Guo, H. et al. Transparent, flexible, and stretchable WS 2 based humidity sensors for electronic skin. *Nanoscale* **9**, 6246–6253 (2017).
17. Navaraj, W. T., Gupta, S., Lorenzelli, L. & Dahiya, R. Wafer scale transfer of ultrathin silicon chips on flexible substrates for high performance bendable systems. *Adv. Electron. Mater.* **4**, 1700277 (2018).
18. Sekitani, T., Zschieschang, U., Klauk, H. & Someya, T. Flexible organic transistors and circuits with extreme bending stability. *Nat. Mater.* **9**, 1015 (2010).
19. Kaltenbrunner, M. et al. An ultra-lightweight design for imperceptible plastic electronics. *Nature* **499**, 458 (2013).
20. Viventi, J. et al. Flexible. foldable. actively multiplexed. high-density electrode array for mapping brain activity in vivo. *Nat. Neurosci.* **14**, 1599 (2011).
21. Xu, S. et al. Soft microfluidic assemblies of sensors, circuits, and radios for the skin. *Science* **344**, 70–74 (2014).
22. Imani, S. et al. A wearable chemical-electrophysiological hybrid biosensing system for real-time health and fitness monitoring. *Nat. Commun.* **7**, 11650 (2016).
23. Takei, K., Honda, W., Harada, S., Arie, T. & Akita, S. Toward flexible and wearable human-interactive health-monitoring devices. *Adv. Healthc. Mater.* **4**, 487–500 (2015).
24. Patel, S., Park, H., Bonato, P., Chan, L. & Rodgers, M. A review of wearable sensors and systems with application in rehabilitation. *J. Neuroeng. Rehabil.* **9**, 21 (2012).
25. Fan, F. R. et al. Transparent triboelectric nanogenerators and self-powered pressure sensors based on micropatterned plastic films. *Nano. Lett.* **12**, 3109–3114 (2012).
26. Armand, M. & Tarascon, J. M. Building better batteries. *Nature* **451**, 652 (2008).
27. Wang, Z. L. & Wu, W. Nanotechnology-enabled energy harvesting for self-powered micro-/nanosystems. *Angew. Chem. Int. Ed.* **51**, 11700–11721 (2012).
28. Lipomi, D. J., Tee, B. C. K., Vosgueritchian, M. & Bao, Z. Stretchable organic solar cells. *Adv. Mater.* **23**, 1771–1775 (2011).
29. Lipomi, D. J. & Bao, Z. Stretchable. elastic materials and devices for solar energy conversion. *Energ. Environ. Sci.* **4**, 3314–3328 (2011).
30. Huang, L. et al. Paper electrodes coated with partially-exfoliated graphite and polypyrrole for high-performance flexible supercapacitors. *Polymers* **10**, 135 (2018).
31. Han, S. et al. Battery-free. wireless sensors for full-body pressure and temperature mapping. *Sci. Transl. Med.* **10**, 4950 (2018).
32. Ringeisen, B. R. et al. High power density from a miniature microbial fuel cell using Shewanella oneidensis DSP10. *Environ. Sci. Technol.* **40**, 2629–2634 (2006).
33. Togo, M., Takamura, A., Asai, T., Kaji, H. & Nishizawa, M. An enzyme-based microfluidic biofuel cell using vitamin K3-mediated glucose oxidation. *Electrochim. Acta* **52**, 4669–4674 (2007).
34. Falk, M. et al. Biofuel cell as a power source for electronic contact lenses. *Biosens. Bioelectron.* **37**, 38–45 (2012).
35. Kaltenbrunner, M. et al. Flexible high power-per-weight perovskite solar cells with chromium oxide–metal contacts for improved stability in air. *Nat. Mater.* **14**, 1032 (2015).
36. Khan, S., Dahiya, R. S. & Lorenzelli, L. In *Proc. 44th European Solid State Dev. Res. Conf. (ESSDERC)* 86–89 (IEEE, Venice, 2014).
37. Fan, F. R., Tian, Z. Q. & Wang, Z. L. Flexible triboelectric generator. *Nano Energy* **1**, 328–334 (2012).
38. Manjakkal, L., García Núñez, C., Dang, W. & Dahiya, R. Flexible self-charging supercapacitor based on graphene-Ag-3D graphene foam electrodes. *Nano Energy* **51**, 604–612 (2018).
39. Someya, T. et al. A large-area. flexible pressure sensor matrix with organic field-effect transistors for artificial skin applications. *Proc. Natl Acad. Sci. USA* **101**, 9966–9970 (2004).
40. Hakim, M. M. A. et al. Low cost mass manufacturable silicon nano-sensors for detection of molecules in gas phase. *SF J. Nanochem. Nanotechnol.* **1**, 1006 (2018).
41. Suarez, F., Nozariasbmarz, A., Vashaee, D. & Ozturk, M. C. Designing thermoelectric generators for self-powered wearable electronics. *Energ. Environ. Sci.* **9**, 2099–2113 (2016).
42. Ho, D. H. et al. Stretchable and multimodal all graphene electronic skin. *Adv. Mater.* **28**, 2601–2608 (2016).
43. Bandodkar, A. J. & Wang, J. Non-invasive wearable electrochemical sensors: a review. *Trends Biotechnol.* **32**, 363–371 (2014).
44. Bai, P. et al. Integrated multilayered triboelectric nanogenerator for harvesting biomechanical energy from human motions. *ACS Nano* **7**, 3713–3719 (2013).
45. Yang, Y. et al. Triboelectric nanogenerator for harvesting wind energy and as self-powered wind vector sensor system. *ACS Nano* **7**, 9461–9468 (2013).
46. Wang, Z. L. Triboelectric nanogenerators as new energy technology for self-powered systems and as active mechanical and chemical sensors. *ACS Nano* **7**, 9533–9557 (2013).
47. Min, G., Manjakkal, L., Mulvihill, D. M. & Dahiya, R. Enhanced triboelectric nanogenerator performance via an optimised low permittivity. In *Proc. IEEE Sens. Conf.* (IEEE, Delhi, 2018).
48. Shi, M. et al. Self-powered analogue smart skin. *ACS Nano* **10**, 4083–4091 (2016).
49. Dahiya, R. Valle, M. *Robotic Tactile Sensing* (Springer Publishing, New York, 2013).
50. Dahiya, R., Metta, G., Valle, M. & Sandini, G. Tactile sensing-from humans to humanoids. *IEEE Trans. Robot.* **26**, 1–20 (2010).
51. Dahiya, R., Mittendorfer, P., Valle, M., Cheng, G. & Lumelsky, V. J. Directions toward effective utilization of tactile skin: A review. *Ieee. Sens. J.* **13**, 4121–4138 (2013).
52. Dahiya, R., Navaraj, W. T., Khan, S. & Polat, E. O. Developing electronic skin with sense of touch. *Info Disp.* **31**, 6–10 (2015).

53. Schmitz, A. et al. Methods and technologies for the implementation of large-scale robot tactile sensors. *IEEE Trans. Robot.* **27**, 389–400 (2011).
54. Leonov, V. & Vullers, R. J. M. Wearable electronics self-powered by using human body heat: The state of the art and the perspective. *J. Renew. Sustain. Ener.* **1**, 062701 (2009).
55. Yang, R., Qin, Y., Li, C., Zhu, G. & Wang, Z. L. Converting biomechanical energy into electricity by a muscle-movement-driven nanogenerator. *Nano. Lett.* **9**, 1201–1205 (2009).
56. Li, C. et al. Wearable energy-smart ribbons for synchronous energy harvest and storage. *Nat. Commun.* **7**, 13319 (2016).
57. Hammock, M. L., Chortos, A., Tee, B. C. K., Tok, J. B. H. & Bao, Z. 25th anniversary article: the evolution of electronic skin (*e*-skin): a brief history, design considerations, and recent progress. *Adv. Mater.* **25**, 5997–6038 (2013).
58. Chortos, A., Liu, J. & Bao, Z. Pursuing prosthetic electronic skin. *Nat. Mater.* **15**, 937 (2016).
59. Fraunhofer, I. *Photovoltaics report* (Fraunhofer ISE, Freiburg, 2016).
60. Ichikawa, Y., Yoshida, T., Hama, T., Sakai, H. & Harashima, K. Production technology for amorphous silicon-based flexible solar cells. *Sol. Energy Mater. Sol. Cells* **66**, 107–115 (2001).
61. Kaltenbrunner, M. et al. Ultrathin and lightweight organic solar cells with high flexibility. *Nat. Commu.* **3**, 770 (2012).
62. Gu, X. et al. Roll-to-roll printed large-area all-polymer solar cells with 5% efficiency based on a low crystallinity conjugated polymer blend. *Adv. Energy Mater.* **7**, 1602742 (2017).
63. Günes, S., Neugebauer, H. & Sariciftci, N. S. Conjugated polymer-based organic solar cells. *Chem. Rev.* **107**, 1324–1338 (2007).
64. Schubert, M. B. & Werner, J. H. Flexible solar cells for clothing. *Mater. Today* **9**, 42–50 (2006).
65. Hu, X. et al. Wearable large-scale perovskite solar-power source via nanocellular scaffold. *Adv. Mater.* **29**, 1703236 (2017).
66. Green, M. A., Emery, K., Hishikawa, Y., Warta, W. & Dunlop, E. D. Solar cell efficiency tables (Version 45). *Prog. Photovolt. Res. Appl.* **23**, 1–9 (2015).
67. Kayes, B. M. et al. 27.6% conversion efficiency, a new record for single-junction solar cells under 1 sun illumination. In *Proc. 37th IEEE Photovolt. Spec. Conf. (PVSC)* 000004-000008 (IEEE, Seattle, 2011).
68. Yablonovitch, E., Gmitter, T., Harbison, J. & Bhat, R. Extreme selectivity in the lift-off of epitaxial GaAs films. *Appl. Phys. Lett.* **51**, 2222–2224 (1987).
69. O'regan, B. & Grätzel, M. A low-cost. high-efficiency solar cell based on dye-sensitized colloidal TiO_2 films. *Nature* **353**, 737 (1991).
70. Robertson, N. Optimizing dyes for dye-sensitized solar cells. *Angew. Chem. Int. Ed.* **45**, 2338–2345 (2006).
71. Yu, J., Fan, J. & Lv, K. Anatase TiO_2 nanosheets with exposed (001) facets: improved photoelectric conversion efficiency in dye-sensitized solar cells. *Nanoscale* **2**, 2144–2149 (2010).
72. Xie, Y. et al. Porphyrin cosensitization for a photovoltaic efficiency of 11.5%: a record for non-ruthenium solar cells based on iodine electrolyte. *J. Am. Chem. Soc.* **137**, 14055–14058 (2015).
73. Yella, A. et al. Porphyrin-sensitized solar cells with cobalt (II/III)-based redox electrolyte exceed 12 percent efficiency. *Science* **334**, 629–634 (2011).
74. Saito, M. & Fujihara, S. Large photocurrent generation in dye-sensitized ZnO solar cells. *Energ. Environ. Sci.* **1**, 280–283 (2008).
75. Li, L., Zhai, T., Bando, Y. & Golberg, D. Recent progress of one-dimensional ZnO nanostructured solar cells. *Nano Energy* **1**, 91–106 (2012).
76. Lu, J. et al. Well-aligned TiO_2 nanorod arrays prepared by dc reactive magnetron sputtering for flexible dye-sensitized solar cells. *Mater. Lett.* **188**, 323–326 (2017).
77. Jiang, C. et al. High-bendability flexible dye-sensitized solar cell with a nanoparticle-modified ZnO-nanowire electrode. *Appl. Phys. Lett.* **92**, 143101 (2008).
78. Thompson, B. C. & Fréchet, J. M. J. Polymer–fullerene composite solar cells. *Angew. Chem. Int. Ed.* **47**, 58–77 (2008).
79. Tang, C. W. Two-layer organic photovoltaic cell. *Appl. Phys. Lett.* **48**, 183–185 (1986).
80. Brabec, C. J. et al. Polymer–fullerene bulk-heterojunction solar cells. *Adv. Mater.* **22**, 3839–3856 (2010).
81. Gasparini, N. The physics of small molecule acceptors for efficient and stable bulk heterojunction solar cells. *Adv. Energy Mater.* **8**, 1703298 (2018).
82. Shaheen, S. E. et al. 2.5% efficient organic plastic solar cells. *Appl. Phys. Lett.* **78**, 841–843 (2001).
83. Lee, J. Y., Connor, S. T., Cui, Y. & Peumans, P. Semitransparent organic photovoltaic cells with laminated top electrode. *Nano. Lett.* **10**, 1276–1279 (2010).
84. Bailie, C. D. et al. Semi-transparent perovskite solar cells for tandems with silicon and CIGS. *Energ. Environ. Sci.* **8**, 956–963 (2015).
85. Alivisatos, A. P. Semiconductor clusters, nanocrystals, and quantum dots. *Science* **271**, 933–937 (1996).
86. Santra, P. K. & Kamat, P. V. Mn-doped quantum dot sensitized solar cells: a strategy to boost efficiency over 5%. *J. Am. Chem. Soc.* **134**, 2508–2511 (2012).
87. Dayal, S., Kopidakis, N., Olson, D. C., Ginley, D. S. & Rumbles, G. Photovoltaic devices with a low band gap polymer and CdSe nanostructures exceeding 3% efficiency. *Nano. Lett.* **10**, 239–242 (2010).
88. Deng, M. et al. Low-cost flexible nano-sulfide/carbon composite counter electrode for quantum-dot-sensitized solar cell. *Nanoscale Res. Lett.* **5**, 986 (2010).
89. Liu, D. & Kelly, T. L. Perovskite solar cells with a planar heterojunction structure prepared using room-temperature solution processing techniques. *Nat. Photon.* **8**, 133 (2014).
90. Xu, B. et al. Carbazole-based hole-transport materials for efficient solid-state dye-sensitized solar cells and perovskite solar cells. *Adv. Mater.* **26**, 6629–6634 (2014).
91. Yoon, H., Kang, S. M., Lee, J.-K. & Choi, M. Hysteresis-free low-temperature-processed planar perovskite solar cells with 19.1% efficiency. *Energ. Environ. Sci.* **9**, 2262–2266 (2016).
92. Luo, Q. et al. All-carbon-electrode-based endurable flexible perovskite solar cells. *Adv. Funct. Mater.* **28**, 1706777 (2018).
93. Yang, D. et al. Hysteresis-suppressed high-efficiency flexible perovskite solar cells using solid-state ionic-liquids for effective electron transport. *Adv. Mater.* **28**, 5206–5213 (2016).
94. Roundy, S. et al. Improving power output for vibration-based energy scavengers. *IEEE Pervas. Compu.* **4**, 28–36 (2005).
95. Ali, S., Friswell, M. & Adhikari, S. Analysis of energy harvesters for highway bridges. *J. Intell. Mater. Syst. Struct.* **22**, 1929–1938 (2011).
96. Ahmad, A., Khan, Z. A., Saad Alam, M. & Khateeb, S. A review of the electric vehicle charging techniques. standards. progression and evolution of EV technologies in Germany. *Smart Sci.* **6**, 36–53 (2018).
97. Wang, Y., Yang, Y. & Wang, Z. L. Triboelectric nanogenerators as flexible power sources. *NPJ Flex. Electron.* **1**, 10 (2017).
98. El-Hami, M. et al. Design and fabrication of a new vibration-based electromechanical power generator. *Sens. Actuator A-Phys.* **92**, 335–342 (2001).
99. Glynne-Jones, P. & White, N. M. Self-powered systems: a review of energy sources. *Sens. Rev.* **21**, 91–98 (2001).
100. Beeby, S. P. et al. A micro electromagnetic generator for vibration energy harvesting. *J. Micromech. Microeng.* **17**, 1257 (2007).
101. Wang, Z. L. & Song, J. Piezoelectric nanogenerators based on zinc oxide nanowire arrays. *Science* **312**, 242–246 (2006).
102. Gao, P. X., Song, J., Liu, J. & Wang, Z. L. Nanowire piezoelectric nanogenerators on plastic substrates as flexible power sources for nanodevices. *Adv. Mater.* **19**, 67–72 (2007).
103. Xu, S. et al. Self-powered nanowire devices. *Nat. Nanotech.* **5**, 366 (2010).
104. Shen, D. et al. Micromachined PZT cantilever based on SOI structure for low frequency vibration energy harvesting. *Sens. Actuator A-Phys.* **154**, 103–108 (2009).
105. Gao, Y. & Wang, Z. L. Electrostatic potential in a bent piezoelectric nanowire. The fundamental theory of nanogenerator and nanopiezotronics. *Nano. Lett.* **7**, 2499–2505 (2007).
106. Gao, Z. et al. Effects of piezoelectric potential on the transport characteristics of metal-ZnO nanowire-metal field effect transistor. *J. Appl. Phys.* **105**, 113707 (2009).
107. Liu, J. et al. Carrier density and Schottky barrier on the performance of DC nanogenerator. *Nano. Lett.* **8**, 328–332 (2008).
108. Huang, Y. Logic gates and computation from assembled nanowire building blocks. *Science* **294**, 1313–1317 (2001).
109. Lin, Y. F., Song, J., Ding, Y., Lu, S. Y. & Wang, Z. L. Piezoelectric nanogenerator using CdS nanowires. *Appl. Phys. Lett.* **92**, 022105 (2008).
110. Huang, C. T. et al. Single-InN-nanowire nanogenerator with upto 1 V output voltage. *Adv. Mater.* **22**, 4008–4013 (2010).
111. Huang, C. T. et al. GaN nanowire arrays for high-output nanogenerators. *J. Am. Chem. Soc.* **132**, 4766–4771 (2010).
112. Wang, X., Song, J., Liu, J. & Wang, Z. L. Direct-current nanogenerator driven by ultrasonic waves. *Science* **316**, 102–105 (2007).
113. Xu, S., Wei, Y., Liu, J., Yang, R. & Wang, Z. L. Integrated multilayer nanogenerator fabricated using paired nanotip-to-nanowire brushes. *Nano. Lett.* **8**, 4027–4032 (2008).
114. Bai, S. et al. Single crystalline lead zirconate titanate (PZT) nano/micro-wire based self-powered UV sensor. *Nano Energy* **1**, 789–795 (2012).
115. Zhu, G., Yang, R., Wang, S. & Wang, Z. L. Flexible high-output nanogenerator based on lateral ZnO nanowire array. *Nano. Lett.* **10**, 3151–3155 (2010).
116. Hu, Y., Zhang, Y., Xu, C., Zhu, G. & Wang, Z. L. High-output nanogenerator by rational unipolar assembly of conical nanowires and its application for driving a small liquid crystal display. *Nano. Lett.* **10**, 5025–5031 (2010).
117. Yang, R., Qin, Y., Dai, L. & Wang, Z. L. Power generation with laterally packaged piezoelectric fine wires. *Nat. Nanotech.* **4**, 34 (2008).

118. Li, Z., Zhu, G., Yang, R., Wang, A. C. & Wang, Z. L. Muscle-driven in vivo nanogenerator. *Adv. Mater.* **22**, 2534–2537 (2010).
119. Qin, Y., Wang, X. & Wang, Z. L. Microfibre–nanowire hybrid structure for energy scavenging. *Nature* **451**, 809 (2008).
120. Li, Z. & Wang, Z. L. Air/liquid-pressure and heartbeat-driven flexible fiber nanogenerators as a micro/nano-power source or diagnostic sensor. *Adv. Mater.* **23**, 84–89 (2011).
121. Wang, S., Lin, L. & Wang, Z. L. Nanoscale triboelectric-effect-enabled energy conversion for sustainably powering portable electronics. *Nano. Lett.* **12**, 6339–6346 (2012).
122. Zhu, G. et al. Toward large-scale energy harvesting by a nanoparticle-enhanced triboelectric nanogenerator. *Nano. Lett.* **13**, 847–853 (2013).
123. Wang, S. Sliding-triboelectric nanogenerators based on in-plane charge-separation mechanism. *Nano. Lett.* **13**, 2226–2233 (2013).
124. Zhang, X. S. et al. Frequency-multiplication high-output triboelectric nanogenerator for sustainably powering biomedical microsystems. *Nano. Lett.* **13**, 1168–1172 (2013).
125. Zhu, G. et al. Linear-grating triboelectric generator based on sliding electrification. *Nano. Lett.* **13**, 2282–2289 (2013).
126. Lin, L. et al. Segmentally structured disk triboelectric nanogenerator for harvesting rotational mechanical energy. *Nano. Lett.* **13**, 2916–2923 (2013).
127. Yang, Y. A single-electrode based triboelectric nanogenerator as self-powered tracking system. *Adv. Mater.* **25**, 6594–6601 (2013).
128. Minnich, A. J., Dresselhaus, M. S., Ren, Z. F. & Chen, G. Bulk nanostructured thermoelectric materials: current research and future prospects. *Energ. Environ. Sci.* **2**, 466–479 (2009).
129. Koukharenko, E. et al. Towards thermoelectric nanostructured energy harvester for wearable applications. *J. Mater. Sci. Mater. Electron.* **29**, 3423–3436 (2018).
130. Brown, S. R., Kauzlarich, S. M., Gascoin, F. & Snyder, G. J. $Yb_{14}MnSb_{11}$: new high efficiency thermoelectric material for power generation. *Chemi. Mater.* **18**, 1873–1877 (2006).
131. Tang, X., Zhang, Q., Chen, L., Goto, T. & Hirai, T. Synthesis and thermoelectric properties of p-type- and n-type-filled skutterudite $R_yM_xCo_{4-x}Sb_{12}$(R:Ce,Ba,Y;M: Fe,Ni). *J. Appl. Phys.* **97**, 093712 (2005).
132. Saramat, A. et al. Large thermoelectric figure of merit at high temperature in Czochralski-grown clathrate $Ba_8Ga_{16}Ge_{30}$. *J. Appl. Phys.* **99**, 023708 (2006).
133. Venkatasubramanian, R., Siivola, E., Colpitts, T. & O'Quinn, B. Thin-film thermoelectric devices with high room-temperature figures of merit. *Nature* **413**, 597 (2001).
134. Chung, D. Y. et al. $CsBi_4Te_6$: a high-performance thermoelectric material for low-temperature applications. *Science* **287**, 1024–1027 (2000).
135. Szczech, J. R., Higgins, J. M. & Jin, S. Enhancement of the thermoelectric properties in nanoscale and nanostructured materials. *J. Mater. Chem.* **21**, 4037–4055 (2011).
136. Lin, Y. M. & Dresselhaus, M. Thermoelectric properties of superlattice nanowires. *Phys., Rev. B* **68**, 075304 (2003).
137. Zhang, G., Yu, Q., Wang, W. & Li, X. Nanostructures for thermoelectric applications: synthesis. growth mechanism, and property studies. *Adv. Mater.* **22**, 1959–1962 (2010).
138. Zhao, X. B. Bismuth telluride nanotubes and the effects on the thermoelectric properties of nanotube-containing nanocomposites. *Appl. Phys. Lett.* **86**, 062111 (2005).
139. Alhawari, M., Mohammad, B., Saleh, H. & Ismail, M. *Energy Harvesting for Self-Powered Wearable Devices*. (Springer, Berlin, Germany, 2018).
140. Mount, L. T. in *Heat loss from animals and man* 425–439 (Butterworth & Co, London, 1974).
141. Torfs, T. Pulse oximeter fully powered by human body heat. *Sens. Transducers J.* **80**, 1230–1238 (2007).
142. Su, J. et al. Thermoelectric energy harvester fabricated by Stepper. *Microelectron. Eng.* **87**, 1242–1244 (2010).
143. Bullen, R. A., Arnot, T., Lakeman, J. & Walsh, F. Biofuel cells and their development. *Biosens. Bioelectron.* **21**, 2015–2045 (2006).
144. Bandodkar, A. J. Wearable biofuel cells: past, present and future. *J. Electrochem. Soc.* **164**, H3007–H3014 (2017).
145. Garcia, S. et al. Wearable sensor system powered by a biofuel cell for detection of lactate levels in sweat. *ECS J. Solid State Sci. Technol.* **5**, M3075 (2016).
146. Xu, Z. et al. Flat enzyme-based lactate biofuel cell integrated with power management system: Towards long term in situ power supply for wearable sensors. *Appl. Energy* **194**, 71–80 (2017).
147. Yeknami, A. F. et al. A 0.3 V biofuel-cell-powered glucose/lactate biosensing system employing a 180 nW 64 dB SNR passive δς ADC and a 920 MHz wireless transmitter. In *Proc. IEEE International Solid State Circuits Conference (ISSCC)* 284–286 (IEEE, San Francisco, 2018).
148. Minteer, S. D., Liaw, B. Y. & Cooney, M. J. Enzyme-based biofuel cells. *Curr. Opin. Biotechnol.* **18**, 228–234 (2007).
149. Southcott, M. et al. A pacemaker powered by an implantable biofuel cell operating under conditions mimicking the human blood circulatory system–battery not included. *Phys. Chem. Chem. Phys.* **15**, 6278–6283 (2013).
150. Sim, H. J. et al. Stretchable fiber biofuel cell by rewrapping multiwalled carbon nanotube sheets. *Nano. Lett.* **18**, 5272–5278 (2018).
151. Jia, W., Valdés-Ramírez, G., Bandodkar, A. J., Windmiller, J. R. & Wang, J. Epidermal biofuel cells: energy harvesting from human perspiration. *Angew. Chem. Int. Ed.* **52**, 7233–7236 (2013).
152. Jia, W. et al. Wearable textile biofuel cells for powering electronics. *J. Mater. Chem. A* **2**, 18184–18189 (2014).
153. Fujimagari, Y. & Nishioka, Y. Stretchable glucose biofuel cell with wirings made of multiwall carbon nanotubes. *J. Phys. Conf. Series* **660**, 012130 (2015).
154. Bandodkar, A. J. et al. Soft. stretchable. high power density electronic skin-based biofuel cells for scavenging energy from human sweat. *Energ. Environ. Sci.* **10**, 1581–1589 (2017).
155. Miyake, T., Haneda, K., Yoshino, S. & Nishizawa, M. Flexible. layered biofuel cells. *Biosens. Bioelectron.* **40**, 45–49 (2013).
156. Jeerapan, I., Sempionatto, J. R., Pavinatto, A., You, J. M. & Wang, J. Stretchable biofuel cells as wearable textile-based self-powered sensors. *J. Mater. Chem. A* **4**, 18342–18353 (2016).
157. Yu, P., Zhao, X., Huang, Z., Li, Y. & Zhang, Q. Free-standing three-dimensional graphene and polyaniline nanowire arrays hybrid foams for high-performance flexible and lightweight supercapacitors. *J. Mater. Chem. A* **2**, 14413–14420 (2014).
158. Guo, K., Ma, Y., Li, H. & Zhai, T. Flexible wire-shaped supercapacitors in parallel double helix configuration with stable electrochemical properties under static/dynamic bending. *Small* **12**, 1024–1033 (2016).
159. Xiong, Z., Liao, C., Han, W. & Wang, X. Mechanically tough large-area hierarchical porous graphene films for high-performance flexible supercapacitor applications. *Adv. Mater.* **27**, 4469–4475 (2015).
160. Yu, C., Masarapu, C., Rong, J., Wei, B. & Jiang, H. Stretchable supercapacitors based on buckled single-walled carbon-nanotube macrofilms. *Adv. Mater.* **21**, 4793–4797 (2009).
161. Meng, C., Liu, C., Chen, L., Hu, C. & Fan, S. Highly flexible and all-solid-state paperlike polymer supercapacitors. *Nano Lett.* **10**, 4025–4031 (2010).
162. Pan, X. et al. Fast supercapacitors based on graphene-bridged V_2O_3/VOx core-shell nanostructure electrodes with a power density of 1 MW kg^{-1}. *Adv. Mater. Interfaces* **1**, 1400398 (2014).
163. Bae, J. et al. Fiber supercapacitors made of nanowire-fiber hybrid structures for wearable/flexible energy storage. *Angew. Chem. Int. Ed.* **50**, 1683–1687 (2011).
164. Fu, Y. et al. Fiber supercapacitors utilizing pen ink for flexible/wearable energy storage. *Adv. Mater.* **24**, 5713–5718 (2012).
165. Rudola, A., Gajjela, S. R. & Balaya, P. High energy density in-situ sodium plated battery with current collector foil as anode. *Electrochem. Commun.* **86**, 157–160 (2018).
166. Lee, Y. H. et al. Wearable textile battery rechargeable by solar energy. *Nano. Lett.* **13**, 5753–5761 (2013).
167. Hu, L., Wu, H., La Mantia, F., Yang, Y. & Cui, Y. Thin, flexible secondary Li-Ion paper batteries. *ACS Nano* **4**, 5843–5848 (2010).
168. Jia, X. et al. High-performance flexible lithium-ion electrodes based on robust network architecture. *Energ. Environ. Sci.* **5**, 6845–6849 (2012).
169. Bao, Y. et al. Free-standing and flexible $LiMnTiO_4$/carbon nanotube cathodes for high performance lithium ion batteries. *J. Power Sources* **321**, 120–125 (2016).
170. Lu, Y. et al. Flexible and free-standing organic/carbon nanotubes hybrid films as cathode for rechargeable lithium-ion batteries. *J. Phys. Chem. C.* **121**, 14498–14506 (2017).
171. Ren, J. et al. Elastic and wearable wire-shaped lithium-ion battery with high electrochemical performance. *Angew. Chem.* **126**, 7998–8003 (2014).
172. Fu, J. et al. Electrically rechargeable zinc–air batteries: progress, challenges, and perspectives. *Adv. Mater.* **29**, 1604685 (2017).
173. Li, Y. et al. Atomically thin mesoporous Co_3O_4 layers strongly coupled with N-rGO nanosheets as high-performance bifunctional catalysts for 1D knittable zinc-air batteries. *Adv. Mater.* **30**, 1703657 (2017).
174. Kaltenbrunner, M., Kettlgruber, G., Siket, C., Schwödiauer, R. & Bauer, S. Arrays of ultracompliant electrochemical dry gel cells for stretchable electronics. *Adv. Mater.* **22**, 2065–2067 (2010).
175. Agbinya, J. I. *Wireless Power Transfer* Vol. 45 (River Publishers, 2015).
176. Li, L., Liu, H., Zhang, H. & Xue, W. Efficient wireless power transfer system integrating with metasurface for biological applications. *IEEE Trans. Ind. Electron.* **65**, 3230–3239 (2018).
177. Jadidian, J. & Katabi, D. Wireless power transfer. U.S. Patent No. 9,800,076 (2017).
178. Aqueveque, P. & Barboza, J. Wireless power system for charge supercapacitors as power sources for implantable devices. In *Proc. IEEE PELS Workshop Emerging Technol. Wireless Power (WoW)* 1–5 (IEEE, Daejeon, 2015).

179. Heo, E., Choi, K. Y., Kim, J., Park, J. H. & Lee, H. A wearable textile antenna for wireless power transfer by magnetic resonance. *Text. Res. J.* **88**, 913–921 (2018).
180. Sun, K. et al. An overview of metamaterials and their achievements in wireless power transfer. *J. Mater. Chem. C.* **6**, 2925–2943 (2018).
181. Strommer, E. et al. NFC-enabled wireless charging. In *Proc. IEEE 4th Int. Workshop Near Field Commun. (NFC)* 36–41 (IEEE, Helsinki, 2012).
182. Park, J., Tak, Y., Kim, Y., Kim, Y. & Nam, S. Investigation of adaptive matching methods for near-field wireless power transfer. *IEEE Trans. Antennas Prop.* **59**, 1769–1773 (2011).
183. Xue, R. F., Cheng, K. W. & Je, M. High-efficiency wireless power transfer for biomedical implants by optimal resonant load transformation. *IEEE Trans. Circ. Syst.* **60**, 867–874 (2013).
184. Li, S. & Mi, C. C. Wireless power transfer for electric vehicle applications. *IEEE J. Em. Sel. Top. P.* **3**, 4–17 (2015).
185. Cao, Q. et al. Highly bendable transparent thin-film transistors that use carbon-nanotube-based conductors and semiconductors with elastomeric dielectrics. *Adv. Mater.* **18**, 304–309 (2006).
186. Sun, Y. & Rogers, J. A. Inorganic semiconductors for flexible electronics. *Adv. Mater.* **19**, 1897–1916 (2007).
187. Cao, Q. et al. Medium-scale carbon nanotube thin-film integrated circuits on flexible plastic substrates. *Nature* **454**, 495–500 (2008).
188. Rogers, J. A. et al. Paper-like electronic displays: large-area rubber-stamped plastic sheets of electronics and microencapsulated electrophoretic inks. *Proc. Natl Acad. Sci. USA* **98**, 4835–4840 (2001).
189. Cao, Q. & Rogers, J. A. Ultrathin films of single-walled carbon nanotubes for electronics and sensors: a review of fundamental and applied aspects. *Adv. Mater.* **21**, 29–53 (2009).
190. Navaraj, W. T., Gupta, S., Lorenzelli, L. & Dahiya, R. Wafer scale transfer of ultra-thin silicon chips on flexible substrates for high performance bendable systems. *Adv. Electron. Mater.* **4**, 1700277 (2018).
191. Schwartz, G. et al. Flexible polymer transistors with high pressure sensitivity for application in electronic skin and health monitoring. *Nat. Commun.* **4**, 1859 (2013).
192. Rao, R. K. Electronic skin patch for real time monitoring of cardiac activity and personal health management. U.S. Patent No. 8,734,339 (2014).
193. Wang, X., Gu, Y., Xiong, Z., Cui, Z. & Zhang, T. Silk-molded flexible, ultrasensitive, and highly stable electronic skin for monitoring human physiological signals. *Adv. Mater.* **26**, 1336–1342 (2014).
194. Mu, C. et al. Enhanced piezocapacitive effect in $CaCu_3Ti_4O_{12}$-polydimethylsiloxane composited sponge for ultrasensitive flexible capacitive sensor. *ACS Appl. Nano Mater.* **1**, 274–283 (2018).
195. Ostfeld, A. E., Gaikwad, A. M., Khan, Y. & Arias, A. C. High-performance flexible energy storage and harvesting system for wearable electronics. *Sci. Rep.* **6**, 26122 (2016).
196. Luo, J. et al. Integration of micro-supercapacitors with triboelectric nanogenerators for a flexible self-charging power unit. *Nano Res.* **8**, 3934–3943 (2015).
197. Xue, X. et al. CuO/PVDF nanocomposite anode for a piezo-driven self-charging lithium battery. *Energ. Environ. Sci.* **6**, 2615–2620 (2013).
198. Yang, P. et al. Electrokinetic supercapacitor for simultaneous harvesting and storage of mechanical energy. *ACS Appl. Mater. Interfaces* **10**, 8010–8015 (2018).
199. Jung, S., Lee, J., Hyeon, T., Lee, M. & Kim, D. H. Fabric-based integrated energy devices for wearable activity monitors. *Adv. Mater.* **26**, 6329–6334 (2014).
200. Ahn, J. H. et al. Heterogeneous three-dimensional electronics by use of printed semiconductor nanomaterials. *Science* **314**, 1754–1757 (2006).
201. Strömmer, E. Hillukkala, M. & Ylisaukko-oja, A. in *Wireless Sensors Actor Networks* 131–142 (Springer, Boston, 2007).
202. Chen, J. et al. Networks of triboelectric nanogenerators for harvesting water wave energy: a potential approach toward blue energy. *ACS Nano* **9**, 3324–3331 (2015).
203. Yogeswaran, N. et al. Piezoelectric graphene field effect transistor pressure sensors for tactile sensing. *Appl. Phys. Lett.* **113**, 014102 (2018).
204. Lu, N. & Kim, D. H. Flexible and stretchable electronics paving the way for soft robotics. *Soft Robot.* **1**, 53–62 (2014).
205. Hou, C., Wang, H., Zhang, Q., Li, Y. & Zhu, M. Highly conductive, flexible, and compressible all-graphene passive electronic skin for sensing human touch. *Adv. Mater.* **26**, 5018–5024 (2014).
206. Guo, L. & DeWeerth, S. P. High-density stretchable electronics: toward an integrated multilayer composite. *Adv. Mater.* **22**, 4030–4033 (2010).
207. Song, H. & Lee, M. H. Combing non-epitaxially grown nanowires for large-area electronic devices. *Nanotechnology* **24**, 285302 (2013).
208. García Núñez, C., Navaraj, W. T., Liu, F., Shakthivel, D. & Dahiya, R. Large-area self-assembly of silica microspheres/nanospheres by temperature-assisted dip-coating. *ACS Appl. Mater. Interfaces* **10**, 3058–3068 (2018).
209. Na, S. I., Kim, S. S., Jo, J. & Kim, D. Y. Efficient and flexible ITO-free organic solar cells using highly conductive polymer anodes. *Adv. Mater.* **20**, 4061–4067 (2008).
210. Semonin, O. E. et al. Peak external photocurrent quantum efficiency exceeding 100% via MEG in a quantum dot solar cell. *Science* **334**, 1530–1533 (2011).
211. Dahiya, R. Electronic skin. *XVIII AISEM Annual Conference.* https://doi.org/10.1109/AISEM.2015.7066762 (2015).
212. Fan, Z. et al. Wafer-scale assembly of highly ordered semiconductor nanowire arrays by contact printing. *Nano. Lett.* **8**, 20–25 (2008).
213. Khan, S., Lorenzelli, L. & Dahiya, R. Towards flexible asymmetric MSM structures using Si microwires through contact printing. *Semicond. Sci. Technol.* **32**, 085013 (2017).
214. Liu, X., Long, Y. Z., Liao, L., Duan, X. & Fan, Z. Large-scale integration of semiconductor nanowires for high-performance flexible electronics. *ACS Nano* **6**, 1888–1900 (2012).
215. Yerushalmi, R., Jacobson, Z. A., Ho, J. C., Fan, Z. & Javey, A. Large scale, highly ordered assembly of nanowire parallel arrays by differential roll printing. *Appl. Phys. Lett.* **91**, 203104 (2007).
216. Sankaran, V. A., Gibeau, J. P., Lathrop, J. A. & Bell, C. W. Vertical wireless power transfer system for charging electric vehicles. U.S. Patent No. 9,931,954 (2018).
217. Xu, S. et al. Stretchable batteries with self-similar serpentine interconnects and integrated wireless recharging systems. *Nat. Commun.* **4**, 1543 (2013).
218. García Núñez, C. et al. Heterogeneous integration of contact-printed semiconductor nanowires for high performance devices on large areas. *Microsyst. Nanoeng.* **4**, 22 (2018).
219. Cho, S., Kim, N., Song, K. & Lee, J. Adhesiveless transfer printing of ultrathin microscale semiconductor materials by controlling the bending radius of an elastomeric stamp. *Langmuir* **32**, 7951–7957 (2016).
220. Wang, B. et al. Adaptable silicon–carbon nanocables sandwiched between reduced graphene oxide sheets as lithium ion battery anodes. *ACS Nano* **7**, 1437–1445 (2013).
221. He, J. et al. Hydrogen substituted graphdiyne as carbon-rich flexible electrode for lithium and sodium ion batteries. *Nat. Commun.* **8**, 1172 (2017).
222. Li, H. et al. Enhanced lithium-storage performance from three-dimensional MoS_2 nanosheets/carbon nanotube paper. *Chem. ElectroChem.* **1**, 1118–1125 (2014).
223. Lu, H., Chen, J. & Tian, Q. Wearable high-performance supercapacitors based on Ni-coated cotton textile with low-crystalline Ni-Al layered double hydroxide nanoparticles. *J. Colloid Interface Sci.* **513**, 342–348 (2018).
224. Guo, J. et al. Direct growth of vanadium nitride nanosheets on carbon nanotube fibers as novel negative electrodes for high-energy-density wearable fiber-shaped asymmetric supercapacitors. *J. Power Sources* **382**, 122–127 (2018).
225. Wang, J. et al. Polymorphous supercapacitors constructed from flexible three-dimensional carbonnetwork/polyaniline/MnO_2 composite textiles. *ACS Appl. Mater. Interfaces* **10**, 10851–10859 (2018).
226. Lin, Y. et al. In-situ growth of high-performance all-solid-state electrode for flexible supercapacitors based on carbon woven fabric/ polyaniline/graphene composite. *J. Power Sources* **384**, 278–286 (2018).
227. Zhang, H. et al. Porous $NiCo_2O_4$ nanowires supported on carbon cloth for flexible asymmetric supercapacitor with high energy density. *J. Energy Chem.* **27**, 195–202 (2018).